Master thesis:

Stability assessment of the landside slope cover on clay flood embankments in the Netherlands

By

L.G.W. Stenveld

TU Delft

rps

Rijkswaterstaat
Ministerie van Infrastructuur en Waterstaat

Cover photo: *Breaching of a flood embankment in Zeeland 1953, where the mechanism sliding of the landside slope cover due to wave overtopping was responsible for 187km of flood embankment failure (NOS, sd).*

Master thesis:

Stability assessment of the landside slope cover on flood embankments in the Netherlands

By

L.G.W. Stenveld

Student number:	4718003
	I
Project duration:	August 1st 2020 – June 15th 2021
Thesis committee:	dr. ir. J.P. Aguilar-Lopez, TU Delft, Chairman. ir. S.J.H. Rikkert, TU Delft, Supervisor. dr. ir. M. van Damme, Rijkswaterstaat / TU Delft, Supervisor. ir. J. Van Mechelen, RPS advies- en ingenieursbureau, Supervisor.
Date:	June 15th 2021, Den Haag.

TU Delft rps Rijkswaterstaat *Ministerie van Infrastructuur en Waterstaat*

Preface

In front of you is my master thesis titled: ‘Stability assessment of the landside slope cover on flood embankments in the Netherlands’. With this thesis, I end my time as a student and my master Civil Engineering at the Delft University of Technology. This research has been done in collaboration with The RPS Consultancy and Engineering firm, and Rijkswaterstaat.

The graduation was a challenging but very rewarding learning experience. Therefore I am grateful for the excellent supervision of my committee that consists of Myron, Jeroen, Stephan, and Juan-Pablo. I found it a pleasant cooperation with the right balance between challenging and guiding me throughout the process of my thesis. You also encouraged me to reach out to intern and extern experts in the field of geo-engineering and flooding probability.

Besides the members of my committee, I would like to thank the colleagues at Rijkswaterstaat and RPS Consultancy and Engineering firm for this great time. Everyone was very helpful and interested in the research topic. I am also verry thankful for the opportunity of STOWA to present the outcomes of this research during the Kennis voor Kunde Platform: Grasbekledingen.

I would also like to thank my friends for the sparring and homework sessions, and my parents for supporting me and encouraging me to reach my goals. Finally I also would like to thank Maria for helping me and supporting me during my studies.

Enjoy reading this thesis.

Lars Stenveld

15-6-2021, Den Haag

Abstract

Large parts of the Netherlands are vulnerable to flooding. Due to the great impact that a flood would have for the Dutch society, The flood safety standards are very strict, which means that the required failure probability of flood defences is very low. To keep the flood risk within acceptable limits of the hinterland, flood embankments are assessed on whether the probability of failure matches the stringent norms using the methods and rules which are stated in the legal assessment instrument (WBI). Within the WBI the probability of failure of the flood embankment equals the sum of the probability of occurrence of individual failure mechanism. This thesis specifically focuses on the failure mechanism: sliding of the landside slope cover due to wave overtopping of clay flood embankments. Due to wave overtopping the relative permeable top layer of the clay embankment becomes saturated. This leads to a shallow subsurface flow parallel to the landside slope cover which is unfavourable for the geotechnical stability of the landside slope cover. The stability assessment of this mechanism is currently assessed with the Edelman & Joustra formula. This formula method is not based on a probabilistic or semi-probabilistic analysis and therefore does not give an failure probability. Instead it uses safety factors. Levee managers therefore believe that the outcome is overly conservative (Waterschappen, et al., 2021). This thesis addresses the question: How can the stability assessment of the Edelman & Joustra formula can be optimized for clay flood embankments in the Netherlands within the legal assessment instrument? To answer this question, new semi-probabilistic safety factors were derived based on a full probabilistic assessment of the Edelman and Joustra formula. The outcomes show that the current approach is not always as conservative as is often assumed. Application of the newly derived safety factor allows levee managers to be more flexible in how to account for the contribution of this failure mechanism to the total levee failure probability. The newly developed method therefore prevents unnecessary rejection and over-dimensioning of flood embankments, so the available resources for flood embankment improvements can be used better.

Table of content

1. Introduction

Large parts of the Netherlands are vulnerable to flooding. Protection against high water is therefore vital. Primary flood defences protect the country from flooding from the main rivers, lakes and the sea. The majority of these primary flood defences are flood embankments, with a total length of 3500 km (TAW, 2004). To guarantee the safety of the hinterland, these flood embankments are assessed by methods and rules which are stated in the legal assessment instrument (WBI). Engineers and flood embankment managers apply the methods described in the WBI to determine if the level of safety offered by the flood embankment satisfy the safety norms.

This thesis specifically focuses on the failure mechanism: sliding of the landside slope cover due to wave overtopping of clay flood embankments. When the flood embankment is overtopped by waves water infiltrates into the relative permeable top layer. Over time this layer becomes fully saturated. The water cannot infiltrate in the impermeable core and a shallow subsurface flow parallel to the landside slope cover occurs. This flow is unfavourable for the stability of the landside slope cover, as a result the landside slope cover can fail and trigger the formation of an embankment breach, see Figure 1.

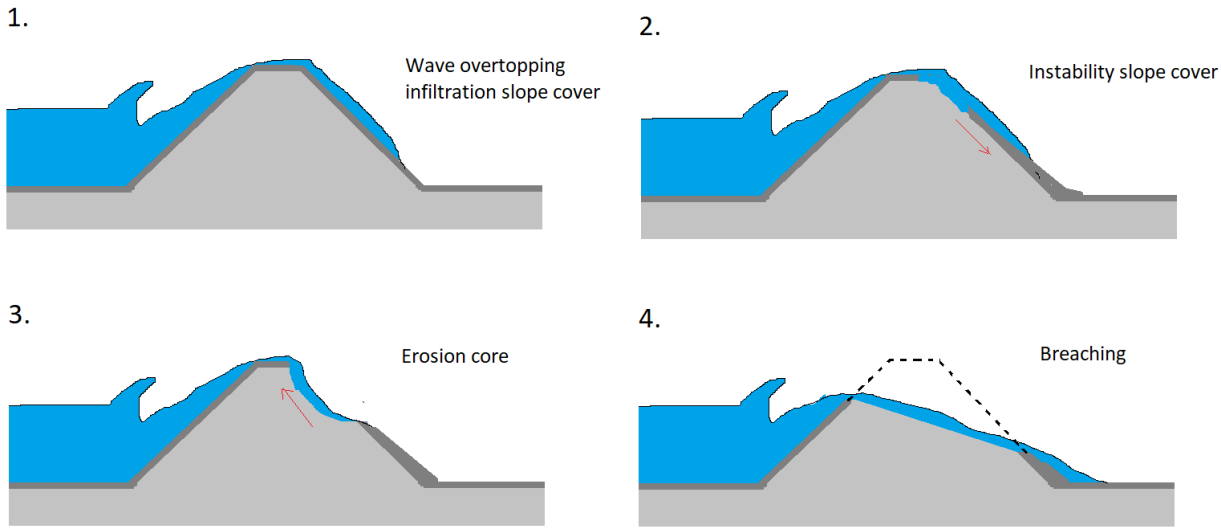

Figure 1 Sliding of the landside slope cover ('t Hart, 2018).

During the flood disaster of 1953, this specific failure mechanism was responsible for the failure of 187 km of flood embankments (Van Hoven et al., 2010). Based on reported damages, Rijkswaterstaat developed a formula to assess the safety of the clay flood embankment which is called the Edelman and Joustra formula, see Equation 1 (Rijkswaterstaat, 1961).

The Edelman & Joustra formula:

Equation 1 Edelman & Joustra

$$SF_{EJ} = \frac{R}{S} = \left[\frac{1}{\gamma_d \cdot \gamma_n}\right] \cdot \frac{\frac{\tan\phi'}{\gamma_{m,\phi}}\left(\frac{\rho_g}{\gamma_{m,\rho}} \cdot g \cdot \cos\alpha - \frac{\rho_w}{\gamma_{m,\rho}} \cdot g\cos\alpha\right) + \frac{c'}{\gamma_{m,c} \cdot d}}{\frac{\rho_g}{\gamma_{m,\rho}} \cdot g \cdot \sin\alpha}$$

tan Ø	Tangent of internal angle of friction	[°]
c	Effective cohesion	[N/m^2]
ρ_g	Density saturated soil	[kg/m^3]
ρ_w	Density water	[kg/m^3]
α	Slope	[°]
g	Gravitational acceleration	[m/s^2]
d	Layer thickness	[m]

The partial safety factors are being used to account for the uncertainty. These factors apply to all clay flood embankments in the Netherlands that are assessed by the Edelman & Joustra formula.

$Y_{m,\phi}$	Partial safety factor tangent Ø	1.1	[-]
$Y_{m,c}$	Partial safety factor *c*	1.25	[-]
Y_d	Model factor	1.1	[-]
Y_n	Damage factor	1.1	[-]

Primary clay flood embankments need to be tested for stability due to overtopping of the landside slope when steeper than 1V:4H and the average overtopping discharge exceeds 0.1 l/s/m, if one of these criteria is not met the stability of the slope is considered safe (Rijkswaterstaat, 2021).

After 60 years the Edelman & Joustra formula is still being used in the current safety assessment (Rijkswaterstaat, 2021). According to this criteria, many clay flood embankments fail the stability assessment. However, flood embankment managers often do not trust the outcome, and they state that the assessment method is overly conservative. In this report, this statement is being reviewed with a probabilistic approach. For this reason, Rijkswaterstaat has asked the author to research if the partial safety factors in the Edelman & Joustra formula can be optimized and develop a semi-probabilistic approach for this mechanism.

1.1 Problem statement

Since 2017, the flood embankment assessment philosophy has changed from an exceedance probability approach to a flooding probability approach. The exceedance probability approach determines whether the load due to the normative water level is greater than the strength of the flood embankment. The flood probability approach takes into account the probability of flooding due to failure of the flood embankment and takes into account the possible consequences of flooding. With this new approach everyone in the Netherlands is offered the same basic level of protection against flooding (Kok & Jongejan, 2016). The mechanism sliding of the landside slope cover has not been upgraded within the flood probability approach and is currently only being assessed if stable or not.

The sliding of the landside slope cover can only occur when the cover is fully saturated due to wave overtopping and there is a critical groundwater flow. Therefore the exceedance probability for an certain overtopping discharge should be taken into account in the safety requirement. In the current stability assessment, there is no difference between a flood embankment with a high exceedance probability of the overtopping discharge and a flood embankment with a low exceedance probability.

The Edelman & Joustra formula has been used for a long time and the results often do not match the expectations of the waterboard managers (Waterschappen, et al., 2021). Therefore the flooding probability approach should be integrated within this stability assessment. With a semi-probabilistic stability assessment, engineers and waterboard managers can apply case-specific hydraulic loads resulting in a truthful stability assessment. With a more accurate stability assessment unnecessary rejection and over dimensioning of flood embankments is avoided, so the available resources for flood embankment improvements can be used better.

1.2 Research scope

Within the main mechanism sliding of the landside slope cover due to wave overtopping, the flood embankment is assessed on different mechanisms depending on the material of the flood embankment, see Table 1.

Table 1 Failure mechanism based on a material of the flood embankment

Type flood embankment	**Failure mechanism**
Clay	Sliding of the landside slope cover
Sand	Washing out of sand particles
Sand core with a clay cover	Uplift of the clay cover, sliding of the landside slope cover, washing out of sand particles.

This research focuses on evaluating the clay flood embankments with the stability assessment of the Edelman & Joustra formula. Only on clay flood embankments the infiltration leads to a critical groundwater flow parallel to the landside slope, which causes the sliding of the landside slope cover (Deltares, 2010). The infiltration tests are used to validate the Spencer-Van der Meij method in D-stability and the Edelman & Joustra formula, cases are generated for the probabilistic analysis.

1.3 Research objectivee

The goal of this research is to evaluate whether optimization of the partial safety factors in the Edelman & Joustra formula is possible and develop a semi-probabilistic approach to evaluate the stability of the landside slope cover for clay flood embankments in the Netherlands.

1.4 Research questions

In line with the research objective the following research question has been defined.

Research question

How can the stability assessment of the Edelman & Joustra formula be optimized for clay flood embankments in the Netherlands within the legal assessment instrument?

Sub questions

1. Is the Spencer-Van der Meij method in D-stability able to reproduce the experimental outcomes from the infiltration tests?

2. How can the model parameters from the Edelman & Joustra formula be derived?

3. Which probabilistic calibration analyses can best be used to derive the partial safety factors for the Edelman Joustra Criterion – the Code calibration from the WBI or Eurocode?

4. How does the selected probabilistic analyses need to be applied to derive the safety factors?

5. What are the optimal safety factors for the Edelman & Joustra formula?

1.5 Research methodology

This thesis focuses on the stability assessment of the landside slope cover with the Edelman & Joustra formula. Chapter 2 focuses on the background information and literature study, Chapter 3 focuses on the stability- and probabilistic analysis, Chapter 4 on the results from these analyses, and Chapters 5 & 6 the research questions are answered.

Background and literature

Chapter 2: Introduces the failure mechanism sliding of the landside slope cover due to wave overtopping. Then the stability assessment by means of the Edelman & Joustra formula and its principles are explained. This will be followed up by an explanation of the slip plane method by Spencer-Van der Meij. Furthermore the process of the infiltration experiments are described, also the data that is collected during these tests have been summarized. In the probabilistic background part, the explanation of the failure probability approach in the Netherlands is explained. This chapter ends by explaining the different types of safety factors and why a certain type is incorporated into the legal assessment instrument (WBI) in the Netherlands.

Stability & probabilistic analysis

Chapter 3: In this chapter the experimental outcomes from the four infiltration tests are reproduced with the Spencer-van der Meij method in the program D-stability. From every infiltration experiment, 10 synthetic cases have been generated with the Latin Hypercube sampling method. The stability factors of these cases are calculated with the Spencer-Van der Meij method in D-stability and the Edelman & Joustra formula in Microsoft excel. The results of both methods are compared, and the model parameters of the Edelman & Joustra formula are determined.

The choice is made which calibration method can best be applied to derive the safety factors. The safety requirement at cross-sectional level is calculated for all infiltration locations; taking into account the exceedance probability of wave overtopping, trajectory norms, the length effect, and the failure budget for sliding of the landside slope cover. This average safety requirement is used as target reliability. The influence coefficients of the parameters in the Edelman & Joustra formula are calculated with the First Order Reliability Method. The safety-in-dependent factors are derived based on the target reliability, the influence coefficients, and the characteristic values. The safety-dependent factor is determined based on the relation between the stability factor and the reliability index.

Results

Chapter 4: In this chapter the results from the data generation, the stability- and probabilistic analysis are presented.

2. Literature

This chapter explains the background of the stability and probabilistic methods and the principles used in this thesis. The chapter has been split into two sections: the stability and the probabilistic literature.

2.1 Stability

In this section, the failure mechanism sliding of the landside slope cover due to wave overtopping is introduced. Then the stability assessment by means of the Edelman & Joustra formula and its principles are explained. This is followed by an explanation of the slip plane method by Spencer-Van der Meij and Bishop.

2.1.1 Sliding of the landside slope cover

In this section a more in-depth view is given on the failure mechanism sliding of the landside slope cover on clay flood embankment due to wave overtopping. The top layer of ±1m of a clay flood embankment often has a developed soil structure (Rijkswaterstaat, 2021). This soil structure develops over time, due to roots penetrating the soil, drying of the sun, expansion due to frost, saturation due to rain and wormholes. Due to these processes, the soil structure has a higher permeability than the core of the flood embankment. When the flood embankment is overtopped, water infiltrates into the top layer. Water is unable to infiltrate into the clay core and flows through the top layer, leading to a groundwater flow parallel to the slope surface. Before this parallel groundwater flow appears multiple theoretical phases have been distinguished (Deltares, 2010).

1. Suction stresses in the drained top layer.
2. The water pressure is around 0 kPa or above and the top layer is completely saturated. The groundwater flow has a gradient directed to the core of the flood embankment.
3. The groundwater flow reaches an impermeable layer or the phreatic line in the core of the flood embankment, this can lead to an increase in water pressure. The gradient of the groundwater flow is directed parallel to the landside slope cover.

The increasing pore pressure, which develops with the parallel groundwater flow, is unfavourable for the stability of the landside slope cover. As a result, the slope cover can become geotechnically unstable. After sliding has occurred, a crack in the crest of the flood embankment appears leading to more infiltration. Failure of the cover layer then exposes the core of the flood embankment and further erosion leads to a decrease in the crest level and breaching, see Figure 1 (Van der Meer J. , 2008).

2.1.2 The Edelman & Joustra formula

The current stability assessment of the landside slope cover on clay flood embankments starts with determining 2 criteria:

1. The first criterion is to determine whether the gradient of the landside slope cover is steeper than 1V:4H for classification II and III clay or 1V:3H for classification I clay, see Figure 2.
2. The second criterion is to determine whether the discharge due to wave overtopping is larger than 0.1 l/s/m by the norm. This is calculated with the program Hydra-NL according to the WBI.

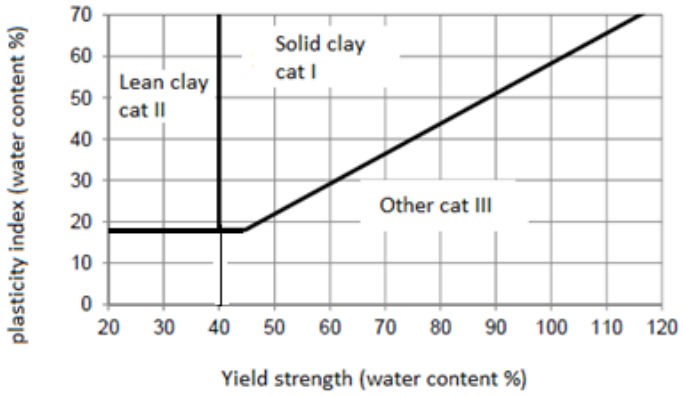

Figure 2 Overview classification of clay (Rijkswaterstaat, 2021).

When both criteria are met, the stability of the landside slope cover due to wave overtopping is assessed with the Edelman & Joustra formula (Rijkswaterstaat, 2021), otherwise, the slope of the flood embankment is considered sufficiently safe.

The Edelman & Joustra formula is based on the following assumptions:

1. The formula uses the drained Mohr-Coulomb parameters, which consist of the cohesion and internal angle of friction. Cohesion is the bonding between soil particles due to electromagnetic bonds and cementation. The internal angle of friction represents the sliding friction and inter partial locking of soil particles, when the normal stresses increases, the friction between the partials increase proportionally.
2. The Edelman & Joustra formula considers the stability equilibrium of a saturated soil layer on an infinitely long slope (Van der Meer et al., 2007). There is a separate correction factor available to take into account the positive effect of the toe, but this is not included in the main formula. More information about this factor is given at the end of end of Section 2.1.2.
3. The schematization only focuses on the geotechnical parameters of the cover layer, the core of the flood embankment is therefore schematized as impermeable and relatively strong.

These assumptions lead to the Edelman & Joustra formula, see Equation 2:

Equation 2 Edelman & Joustra

$$SF_{EJ} = \frac{R}{S} = \left[\frac{1}{\gamma_d \cdot \gamma_n}\right] \cdot \frac{\frac{\tan\phi'}{\gamma_{m,\phi}}\left(\frac{\rho_g}{\gamma_{m,\rho}} \cdot g \cdot \cos\alpha - \frac{\rho_w}{\gamma_{m,\rho}} \cdot g \cos\alpha\right) + \frac{c'}{\gamma_{m,c} \cdot d}}{\frac{\rho_g}{\gamma_{m,\rho}} \cdot g \cdot \sin\alpha}$$

Where:

tan Ø	Tangent of internal angle of friction	[°]
c	Effective cohesion	[N/m^2]
ρ_g	Density saturated soil	[kg/m^3]
ρ_w	Density water	[kg/m^3]
α	Slope	[°]
g	Gravitational acceleration	[m/s^2]
d	Layer thickness	[m]

Safety factors

$Y_{m,\emptyset}$	Partial safety factor tangent Ø	1.1	[-]
$Y_{m,c}$	Partial safety factor *c*	1.25	[-]
Y_d	Model factor	1.1	[-]
Y_n	Damage factor	1.1	[-]

The safety factors in the Edelman & Joustra formula are used to account for parameter uncertainties. The Edelman & Joustra formula considers a stability equilibrium with a driving force and a resisting force. These forces are formulated in the following way and shown in Figure 3:

1. The driving force S is defined as the weight of the saturated cover layer in the downward direction of the landside slope:

$$S = d \cdot \sin\alpha \cdot \rho_g \cdot g$$

2. The resisting force R is defined as the maximum shear strength, which depends on the friction properties and the effective stress on this depth:

$$R = c/d + (\rho_g - \rho_w) \cdot \cos\cdot\ \alpha \cdot\ d\ \cdot tan\emptyset \cdot g$$

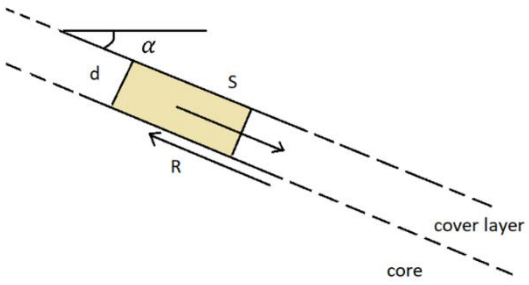

Figure 3 Driving and resisting forces in the Edelman & Joustra criterium. Where: S driving force, R resisting force, d the layer, thickness of the cover and α is angle of the landside slope cover (Van Hoven, Hardeman, Van der Meer, & Steendam, 2010).

The analytical Edelman & Joustra formula considers an infinitely long slope. To account for the positive influence of the toe, the correction factor should be taken into account. This factor is applied to the stability factor when the following criteria are met:

1. The gradient of the slope is smaller than 1V:1.5H.
2. Cohesion should account for more than half of the maximum shear strength.

When these criteria are not met, the correction factor may not be applied.

The correction factor is given in Equation 3.

Equation 3 Correction factor

$$Cr = D^{d/l}$$

Where:

C_r	Correction factor for the toe	[-]
L	Length of the landside slope cover	[m]
d	Thickness of the sliding surface	[m]
D	Constant of: 4.451	[-]

The stability of the landside slope cover is assessed with the Edelman & Joustra formula and the correction factor, when the stability factor is greater than one the landside slope cover is stable and smaller than one the slope is unstable.

2.1.3 Limit equilibrium methods

Besides the Edelman & Joustra criterion, the stability factor can also be calculated with finite element methods (FEM) and limit equilibrium methods (LEM) in combination with a search method to find the most critical slip plane. The engineers and waterboard managers use the LEM methods described by the WBI in the program D-stability. Compared to the FEM the LEM are more time-efficient and give similar results (Javankhoshdel, 2019). The LEM Spencer-Van der Meij is recommended for non-circular slip planes as the sliding of the landside slope cover (Van Hoven, 2016). The method is vulnerable to user input errors and therefore will be controlled with the method of Bishop. Both methods are now briefly described.

Spencer-van der Meij

The Spencer-Van der Meij method is a limit equilibrium method that considers a non-circular slip plane, where the moment-, vertical- and horizontal equilibrium between the slats in the critical slip plane are considered. The metaheuristic search method finds the most critical slip plane on the landside slope cover, see Figure 4 (van Deen, de Bruijn, & Van Duinen, 2019).

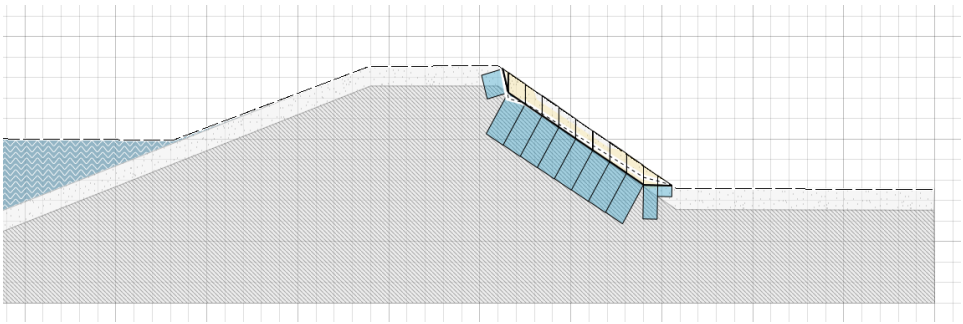

Figure 4 Spencer-Van der Meij calculation in D-stability

Bishop

The Bishop method is a limit equilibrium method that considers a circular slip plane where the moment- and vertical equilibrium are considered. The method considers the maximal shear strength against sliding against the normative driving forces. This method is also combined with a metaheuristic search method to find the most critical slip circle on the slope, see Figure 5 (van Deen, de Bruijn, & Van Duinen, 2019).

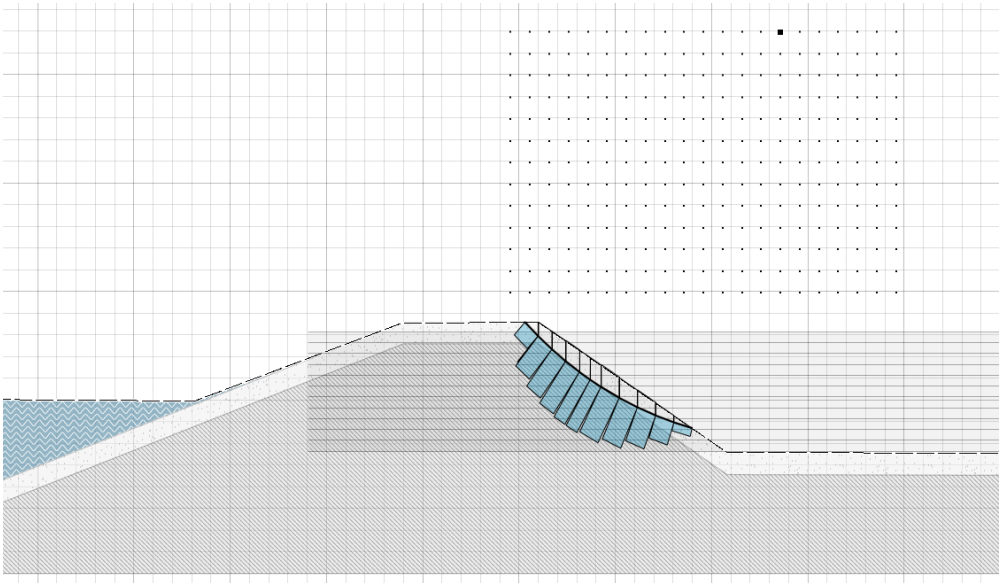

Figure 5 Bishop calculation in D-Stability

2.2 Probabilistics

This section describes the flooding probability approach in the Netherlands, the safety factors and methods to generate cases for the probabilistic analysis.

2.2.1 Flooding probability approach

Before 2017, levee safety assessments were based on the exceedance probability approach. In such an assessment, the hydraulic boundary conditions are determined by an exceedance probability, specified in the flood safety standard. Since 2017, flood defences are assessed on the principle of flood risk (Jongejan, 2017). The flood defence system in the Netherlands is divided into trajectories. For each trajectories, a safety norm has been set based on the consequences of a potential flood of the area protected by the flood embankment. The principle of flood risk here considers the probability that the failure of the flood embankments exceeds the allowable failure probability, set in the norm. The probability of failure due to all possible failure mechanisms and their consequences are considered as a whole see Figure 6. In this figure, sliding of the landside slope cover is indicated by the red circle. This failure mechanism has not been updated to the failure probability approach, and currently the assessment only considers whether the levee is stable or not. Figure 6 gives an overview of the assessed failure mechanisms in a trajectory (Van Hoven, 2016).

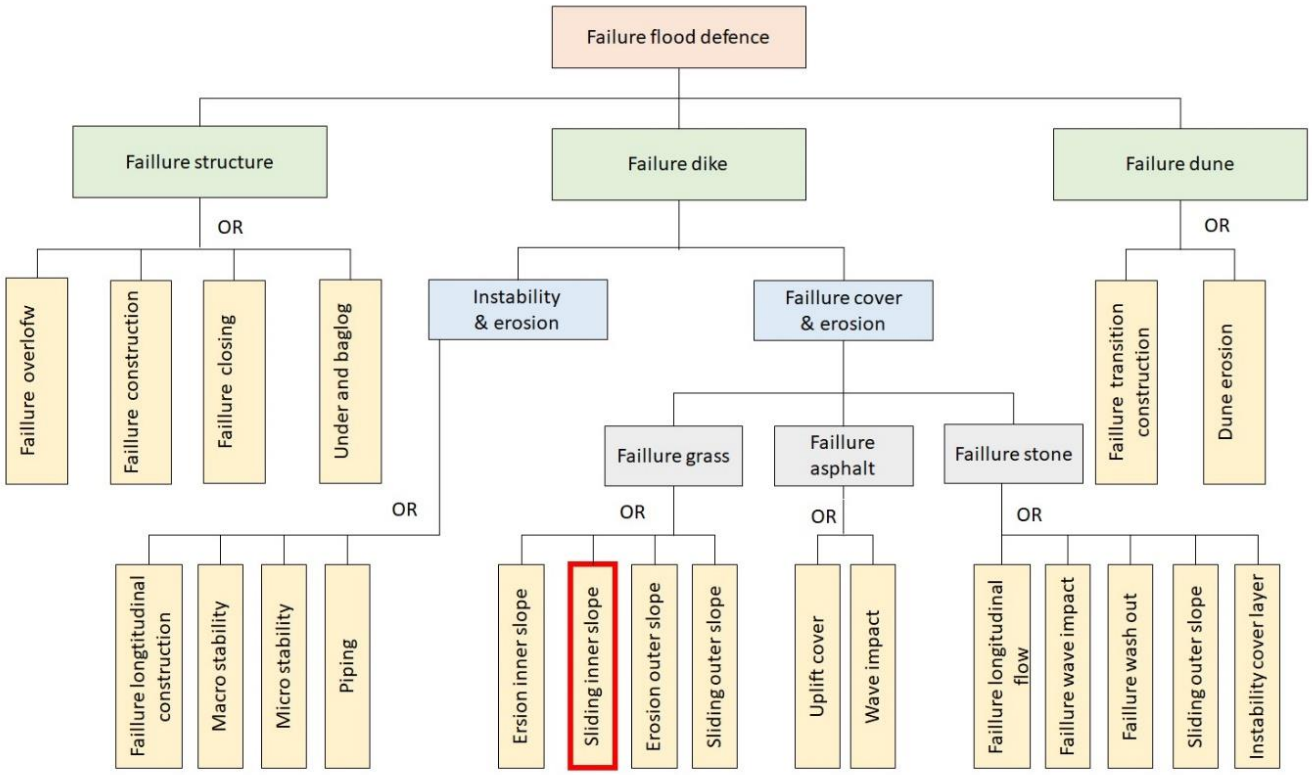

Figure 6 Failure mechanisms in the Netherlands

2.2.2 Partial safety factors

Partial safety factors are commonly used for stability assessments in engineering to describe the uncertainty of a certain parameter. Therefore, the user can assess the stability while taking into account the uncertainty without having to make a full probabilistic calculation. Within the WBI, there are two types of partial safety factors, fixed and variable factors. The fixed partial safety factors are the same for a wide range of values, while the variable factors are dependent on the safety requirement. In general, the variable safety factors lead to a more location specific assessment. Therefore, a semi-probabilistic safety assessment can be used to assess whether a levee meets the safety requirement or not, without giving information about the failure probability, while a full-probabilistic safety assessment results in a failure probability. The advantage of the semi-probabilistic approach with partial safety factors is that it is easy to understand and calculations can be made efficiently facilitating the design processes. Full probabilistic methods can be complex and require numerous calculations. The disadvantage of a semi-probabilistic method is that the assessment is often more conservative than a full-probabilistic assessment which is on the other hand more accurate.

2.2.3 Generation of the data set

As mentioned in the introduction, there have been four infiltration tests on clay flood embankments. To perform a probabilistic analysis to derive a safety method that can be applied for all primary clay flood embankments in the Netherlands, the four infiltration experiments are insufficient and therefore it is required to create a wide range of cases. Algorithms are available for generating these synthetic cases. Two of these methods are briefly discussed now.

Random sampling

The Random Sampling method chooses random values of the parameters, the critical combinations of parameters are within the given statistical distribution. This method is less effective when generating the same amount of samples as with the Latin hypercube sampling, see Figure 8.

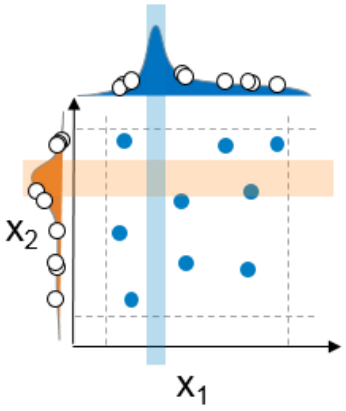

Figure 8 Random sampling

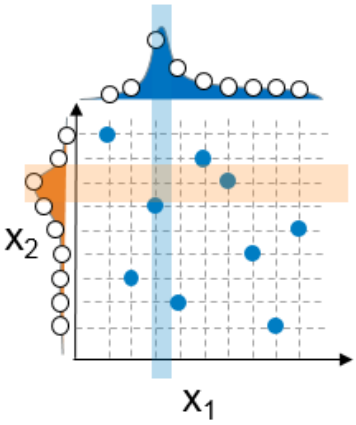

Figure 7 Latin Hypercube sampling

Latin Hypercube Sampling

The Latin Hypercube Sampling method chooses only one value in random blended combinations, therefore a stronger combination can be made from these values. This results in more efficient samples, which more effective than the random sampling method, see Figure 7.

3. Analysis

This chapter describes the dataset and the methods and steps taken in the stability- and the probabilistic analysis.

3.1 Datasets for analysis

Only 4 experimental datasets are available. This is insufficient for a proper statistical analysis. For that reason, additional datasets were generated with the Spencer-van der Meij method in the D-Stability model. From every infiltration test, 10 cases will be generated with the Latin Hypercube sampling algorithm, where the geotechnical parameters will be varied. For their calibration study of macro stability 48 cases were considered (Kanning, et al., 2016). The stability factor of these cases will also be calculated with the Spencer-Van der Meij method in D-stability and the Edelman & Joustra formula in Microsoft excel.

3.1.1 Experimental data

Four infiltration experiments have been performed which are considered suitable for further analysis of GABI. During the infiltration tests, the landside slope cover was constantly covered by a thin layer of water, as can be seen in Figure 9. The experiment aimed to improve the insight into infiltration and its calculation methods. Triggering the sliding of the landside slope cover was not intended, therefore the slope cover was monitored to recognize an early instability so the infiltration can be stopped.

Figure 9 Infiltration experiment near Nieuwerkerk aan den IJssel left and right the infiltration experiment near Gouderak (Noordam & Van Hoven, 2018).

During these infiltration tests, an overtopping discharge of 0.1 l/s/m did not lead to a saturated slope cover, whereas an overtopping discharge of 1.0 l/s/m did lead to a saturated slope cover and a parallel ground water flow on a clay flood embankment (Van Hoven, et al., 2010) and (Noordam & Van Hoven, 2018).

The infiltration experiments were performed on the following locations, see Figure 10.

- Flood embankment, near Delfzijl in February -March 2007 (Akkerman, Van Gerven, & Schaap, 2007).
- Embankment dam the Afsluitdijk near, Kornwederzand in February -March 2009 (Van Hoven, 2010)
- River embankment the IJsseldijk near, Gouderak in August 2017 (Van Hoven, 2017).
- River embankment the Groenendijk near, Nieuwerkerk aan de IJssel in June 2018 (Van der Ruyt, 2018).

Figure 10 Locations infiltration experiments

The following parameters have been measured from these experiments:

- Cross-section profile of the flood embankment
- Geotechnical soil properties from the locations which have been determined from lab tests:

Ø	Internal angle of friction	[°]
c	Cohesion	[kN/m2]
Y_{dry}	Dry unit wait of the material	[kN/m3]
Y_{sat}	Saturated unit wait of the material	[kN/m3]
K	Permeability of the material	[m/s]

- The deformation due to instability obtained from measurement points along the slope
- The phreatic line in the flood embankment measured with pore pressure transducers.
- The discharge of the infiltration experiment given in l/s/m.

During the infiltration test on the IJsseldijk, a shallow shear failure on the landside slope occurred. After the test, a trench was excavated in the slope, where a small sand layer was enclosed between the clay layers. The other cases were stable during the experiments.

3.1.2 Generated data

Additional data points were generated based on four infiltration experiments to facilitate statistical analysis. Therefore, from each existing test, 10 additional cases were generated. This results in a data set consisting of 44 cases, of which 40 cases are synthetic. The amount of cases generated is similar to the calibration analysis for macro stability (Kanning, et al., 2016). The synthetic cases in this thesis were generated with the Latin Hypercube sampling method. The outcome of this method is more valuable than the random sampling method since the random sampling method is only effective when generating a large number of samples. The mean values of the parameters in Table 1 were varied to generate the synthetic cases.

Table 1 Parameters Latin Hypercube sampling

Description		*Unit*	*Distribution*	*Mean*	*Std.*
tan Ø	Internal angle of friction	[°]	normal	Measured*	10%
c	Effective cohesion	[N/m^2]	normal	Measured *	20%
P_g	Density saturated soil	[kg/m^3]	normal	Measured *	5%
d	Layer thickness	[m]	normal	Measured *	10%
α	Gradient slope	[°]	uniform	[1V:1.5H and 1V:4H]	-

Measured *is the measured value in the field at the experiment and is taken as the mean value for each case in the FORM analysis.

The generation of datasets was done using MATLAB, see the complete script in Appendix B. For each infiltration test, 10 synthetic cases were generated for each of the 5 parameters, each parameter was given a value between 0 and 1 by the algorithm. The parameters were then transformed to the inverse cumulative density function, with the mean being the measured value in the experiment and the standard deviation according to (TAW, 2001). The gradient of the landside slope cover was uniformly distributed between 1V:1.5H and 1V:4H.

3.2 Stability analysis

Both the Edelman & Joustra formula as D-Stability were used to analyse the theoretical stability of the slopes

3.2.1 D-Stability

The stability assessment of the cases was executed in the program D-stability, this program is part of the WBI and enables stability analyses to be performed on flood embankments. Each case was manually entered in the program and the steps are briefly elaborated below, for a more in-depth description, see Appendix A Stability calculation.

1. **The geometry of the cross-section.** The cross-section of the flood embankment is entered in the model. For all 43 cases, this consists of a pure clay flood embankment. Only the unstable case of Gouderak consisted of a small sand layer between the clay layers, this is also modelled in the program. The synthetic cases based on Gouderak are modelled as a homogeneous clay profile. The thickness of the cover layer is modelled as a separate layer as has been done for the core, both layers having the same strength parameters, this does not affect the outcome, but the slip planes are easier to define.
2. **Materials:** within the mechanism sliding of the landside slope cover the drained Mohr-Coulomb parameters are applied (Van Hoven, Theorie beoordeling grasbekledingen, 2016). The parameters are the deterministic.
3. **Phreatic level**: In line with the WBI, for all 44 cases the phreatic level has been schematized on the landside slope cover to simulate a fully saturated flood embankment (Rijkswaterstaat, 2021).
4. **Reinforcements**: for the control calculations with the Bishop method, a forbidden line is schematized on the boundary between the cover layer and the core of the flood embankment. The fuction: forbidden line, in D-stability ensures that the critical sliding circle of Bishop does not cut through the boundary, that is defined by the user. By modelling the forbidden line on the boundary layer, the critical slip plane of Bishop only is limited to the cover layer as can be seen in Appendix A, Figure 22.
5. **Calculations**: The stability factor is calculated for both the Spencer-Van der Meij and the Bishop method. Both methods are used in combination with a metaheuristic search method to find the most critical slip plane. The result of the calculation is a stability factor of the most critical slip plane

3.2.2 Edelman & Joustra

The stability assessment with the Edelman & Joustra formula is performed in Microsoft Excel. Here the stability factor is determined including and excluding the partial safety factors.

3.2.3 Determining the model uncertainty of the Edelman & Joustra formula

The mean and standard deviation of the stability factor are determined based on the relation between the stability factor of the Edelman & Joustra and Spencer-Van der Meij. Where the mean is determined with the least squared differences method. The mean and standard deviation of the Edelman & Joustra with respect to the Spencer-Van der Meij has been combined with the mean and standard deviation for the Spencer-Van der Meij from literature (Van Duinen, 2017).

3.3Deriving the safety factors

The goal of the probabilistic analysis is to derive partial safety factor(s) for the Edelman & Joustra formula. Currently, two main calibration methods are available, the method described by the euro code guidelines and the code calibration currently applied in the legal assessment method for various failure mechanisms. The method described by the euro code is considered robust and is conservative, the code calibration currently used in the legal assessment method is considered more refined and consistent with other mechanisms. Therefore the Edelman & Joustra formula has been calibrated with the code calibration method described by (Jongejan, 2017). This method consists of three main steps which have been elaborated in the following sections.

1. Determine the target reliability.
2. Derivation of the safety-dependent factor(s).
3. Derivation of the safety-in-dependent factor.

3.3.1 Determine the target reliability

The first step is to determine the target reliability at the cross-section level for sliding of the landside slope cover due to wave overtopping for each infiltration location. In the current assessment, there is no defined failure budget reserved for sliding of the landside slope cover see Table 2.

Table 2 Maximum allowable failure probabilities per failure mechanism, defined as a percentage of the total failure

Type of flood defense	**Failure mechanism**	**Type of segment**	
		Sandy coast	**Other (levees)**
Levee and structure	Overtopping	0%	24%
Levee	Piping	0%	24%
	Macro instability of the inner slope	0%	4%
	Revetment failure and erosion	0%	10%
Structure	Non-closure	0%	4%
	Piping	0%	2%
	Structural failure	0%	2%
Dune	Dune erosion	70%	0% / 10%*
Other		30%	30 / 20%*
Total		**100%**	**100%**

The failure probability for sliding of the landside slope cover at the cross-section level is based on the maximum allowable flooding probability, the failure budget, length effect, and the exceedance probability of the critical overtopping discharge (Van Hoven, 2019) and (De Visser & Jongejan, 2018). This leads to the following safety requirement, see Equation 4.

Equation 4 Safety requirement at the cross-section

$$P_{T,gabi,q} = \frac{\frac{\omega \cdot P_{max}}{(1 + a \cdot \frac{L}{b})}}{P_{wave(q \geq 1)}}$$

Where:

$P_{T,gabi,q}$	Failure probability requirement for GABI at cross-sectional level.	[-]
ω	Failure budget	[-]
P_{max}	Maximum allowable flooding probability for the trajectory.	[1/year]
a	Fraction of the trajectory length that is sensitive to the considered failure mechanism, default value.	[0.03]
L	Trajectory length	[m]
b	Length independent, equivalent flood embankment sections.	[50]
$P_{wave(q \geq 1)}$	Exceedance probability critical overtopping discharge	[1/year]

Equation 5 Target reliability at the cross-section

$$\beta_{T,gabi,q} = -\Phi^{-1}(P_{T,gabi,q})$$

$\beta_{T,gabi,q}$	Target reliability at the cross-sectional area for sliding off the landside slope cover due to wave overtopping.	[-]
Φ^{-1}	Inverse of the standard normal distribution, where μ:0 and σ:1.	[-]

Failure budget:
Currently, there is no failure budget available for the mechanism sliding of the landside slope cover. Waterboard managers and engineers are allowed to exchange failure budgets between the mechanisms, as long as the total budget for all mechanisms does not exceed 100%. When decreasing the failure budget, this results in a stricter safety requirement. To determine the target reliability a failure budget of 4% from the mechanism macro stability is used, which is in line with (De Visser & Jongejan, 2018).

Length effect:
The length effect of macro stability is chosen over erosion because the quality of the grass cover can be easily inspected, but the spatial variability of the strength parameters not. The mechanism of sliding of the landside slope cover and the mechanism macro stability for shallow slip planes due to wave overtopping are similar.

Critical overtopping discharge
In the current stability assessment, a critical overtopping discharge of 0.1 l/s/m is used. This discharge does not lead to a saturated soil layer based on the infiltration experiments, see Section 3.1. Therefore a critical overtopping discharge of 1.0 l/s/m is chosen based on the experiments and the new critical discharge now also consistent with the assessment of macro stability. This was also discussed within Team Techniek at Rijkswaterstaat, they considered the approach logical but also thought that more research is required to prescribe it in the WBI (Van Damme, et al., 2021).

To determine the exceedance probability of the critical overtopping discharge of 1.0 l/s/m is done in the program Hydra-NL which is currently used in the WBI for determining exceedance probabilities for wave overtopping, see Appendix C for a more detailed step-by-step approach.

3.3.2 Derivation of the safety independent factors.

This chapter consists of three steps which are: 1) Establish a wide range of cases, 2) FORM analysis, and 3) deciding which partial safety factor to include. These steps are now elaborated in more detail.

1) Establish a test set that covers a wide range of cases.

The test set consists of 44 cases which cover a wide range of cases and is representative for clay flood embankments in the Netherlands as discussed in Section 3.1.

2) FORM Analysis

The first-order reliability method (FORM) analysis has been applied to derive the influence coefficients α of the parameters and is calculated in the following way described by (Jonkman, Steenbergen, Morales-Napoles, Vrouwenvelder, & Vrijling, 2017)

Equation 6 Influence coefficients FORM analysis

$$\alpha_{R_i} = \frac{\frac{\partial g_R(r^*)}{\partial R_i}\sigma_{R_i}}{\sqrt{\sum_{i=1}^{m}\left(\frac{\partial g_R(r^*)}{\partial R_i}\cdot\sigma_{R_i}\right)^2 + \sum_{j=1}^{n}\left(\frac{\partial g_E(e^*)}{\partial E_j}\cdot\sigma_{E_j}\right)^2}}$$

The probabilistic analysis is done in the program Prob2B, with the FORM and Crude Monte Carlo Simulation methods, see appendix for a step-by-step description.

The Edelman & Joustra formula consists of the following parameters and their distribution according to the WBI (SH piping, 2019) and (NEN, 2012), see Table 3.

Table 3 Variables probabilistic analysis

	Description	*Unit*	*Distribution*	*Mean*	*Std.*
tan Ø	Internal angle of friction	[°]	normal	Measured*	10%
c	Effective cohesion	[N/m^2]	normal	Measured *	20%
P_g	Density saturated soil	[kg/m^3]	normal	Measured *	5%
P_w	Density water	[kg/m^3]	Deterministic	1031 / 1000*	-
α	Slope	[°]	Deterministic	Measured *	-
g	Gravitational acceleration	[m/s^2]	Deterministic	9.81	-
d	Layer thickness	[m]	normal	1	10%
M	Model uncertainty	[-]	normal	0.96	0.12

- Measured * is the measured value in the field at the experiment and is taken as the mean value for each case in the FORM analysis.
- The density of water differs for salt and fresh water, the cases of Kornwederzand and Delfzijl protect against the sea and Gouderak and Nieuwerkerk aan den IJssel against the river, the synthetic cases are also modelled with the correct values.

3) Derivation of the partial safety factors

This step consists of the derivation of the partial safety factors for the use in the semi-probabilistic assessment, the goal is to select safety factors that are sufficiently safe but not too safe, the latter will result in a conservative assessment.

This can be calculated in the following way according, see Equation 7 and Equation 8 (Jonkman, et al., 2017).

Equation 7 Safety factor for resistance

$$Yr = \frac{\mathrm{u} - \mathrm{k} \cdot \sigma}{\mathrm{u} - \alpha \cdot \beta\mathrm{t} \cdot \sigma}$$

Equation 8 Safety factor for load

$$Ys = \frac{\mathrm{u} - \alpha \cdot \beta\mathrm{t} \cdot \sigma}{\mathrm{u} + \mathrm{k} \cdot \sigma}$$

Where:

Yr	Partial safety factor for resistance*
Ys	Partial safety factor for load*
k	Quantile of reprehensive value Resistance 5% lower bound Load 95% upper bound
u	Mean value
σ	Standard deviation
α	First order reliability method sensitive coefficient
βt	Target reliability index*

Safety factors*: The safety factor for each parameter is the average over the 44 cases, from which 4 are real cases and 40 are synthetic cases.

Target reliability index*: the value for the βt is the average value of the safety requirements for the cross-section of the infiltration locations for the mechanism sliding of the landside slope as elaborated in Section 3.3.1. This differs from the calibration study of macro stability, where the ultimate limit state from the Eurocode is applied (Kanning, et al,. 2016). Failure of the landside slope cover does not directly lead to breach formation, where the ULS considers complete structural failure.

3.3.3 Derivation of the safety dependent factor

In this section, the safety-dependent factor is derived, which reflects the relation between the reliability index and the stability factor, from the Edelman & Joustra formula with the new partial safety factors. The result is a cloud of data points that show the relationship between the factor of safety and the reliability index. With the method of least squared differences, an 80% best fit line can be fitted through the points (Jongejan, 2017). The 80% best fit line means, that 80% of the points lay below this line. This is considered safe but not to safe (Jongejan, 2017) and (Kanning, et al., 2016). The result of the fitted line shows the relation between the stability factor and the target reliability index.

4. Results

This chapter describes the most important results from the stability- and probabilistic analysis which are relevant to answer the sub- and the research questions.

4.1 Stability assessment

This section addresses the following results:

1. The reproduction of the experimental outcomes with the Spencer-Van der Meij and Edelman & Joustra method.
2. The outcomes of the generated dataset with the Latin Hypercube sampling method.
3. The model uncertainty of the Edelman & Joustra formula.

4.1.2 Reproduction experimental outcomes

The experimental outcomes of four experimental test cases are reproduced with the current Edelman & Joustra formula and the Spencer-Van der Meij method according to the methodology described in Section 3.2.1 and 3.2.2, the results from this analysis are shown in Figure 11. For both methods, the partial safety factors are not taken into account. The stability assessment of Edelman & Joustra considers the Gouderak case as stable, while during the experiments the slope was unstable.

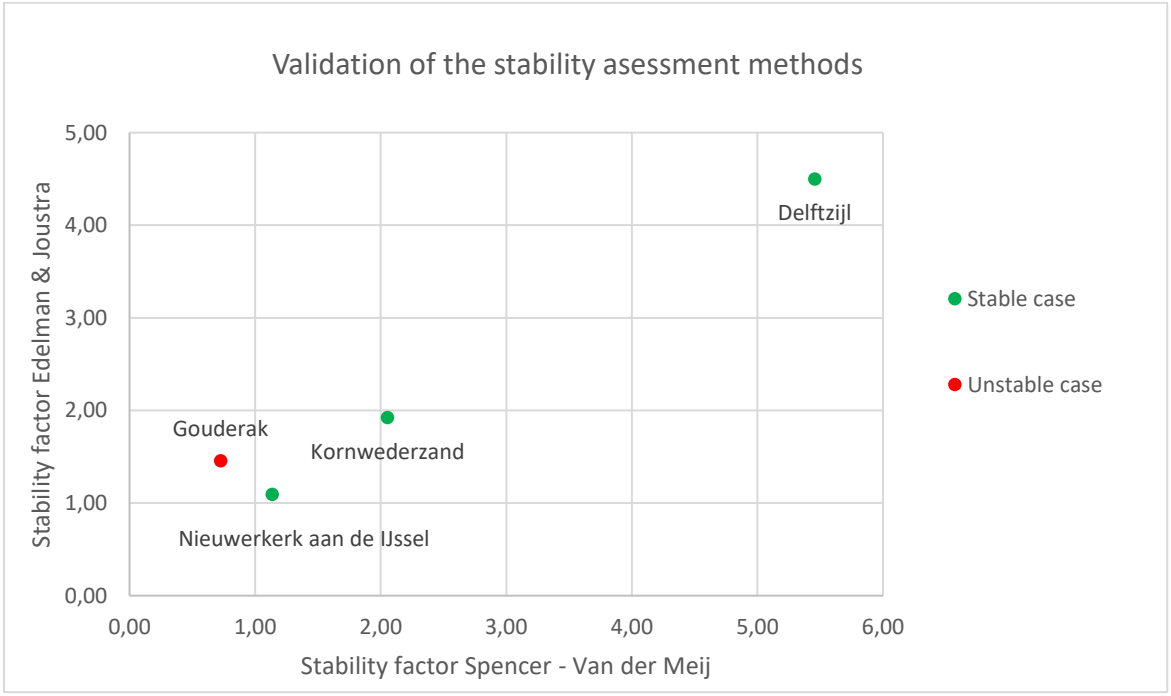

Figure 11 Validation of the Edelman & Joustra- and Spencer-Van der Meij methods with respect to the experimental outcomes, the stable cases are plotted in green, while the unstable case is plotted in red.

4.1.3 Generated cases

The outcome of the generated dataset as described in Section 3.1, is presented in Figure 12. The results of the dataset per location are given in the Appendix B in Table 9, Table 10, Table 11, and Table 12 .The original Gouderak case is modelled with the sand layer situated between the clay core and cover, where all synthetic cases are modelled as homogeneous clay profiles. The spreading of the parameters cohesion, layer thickness, internal angle of friction, and density of the saturated soil are conform the normal distribution, where the values of the gradient of the slope are uniform distributed.

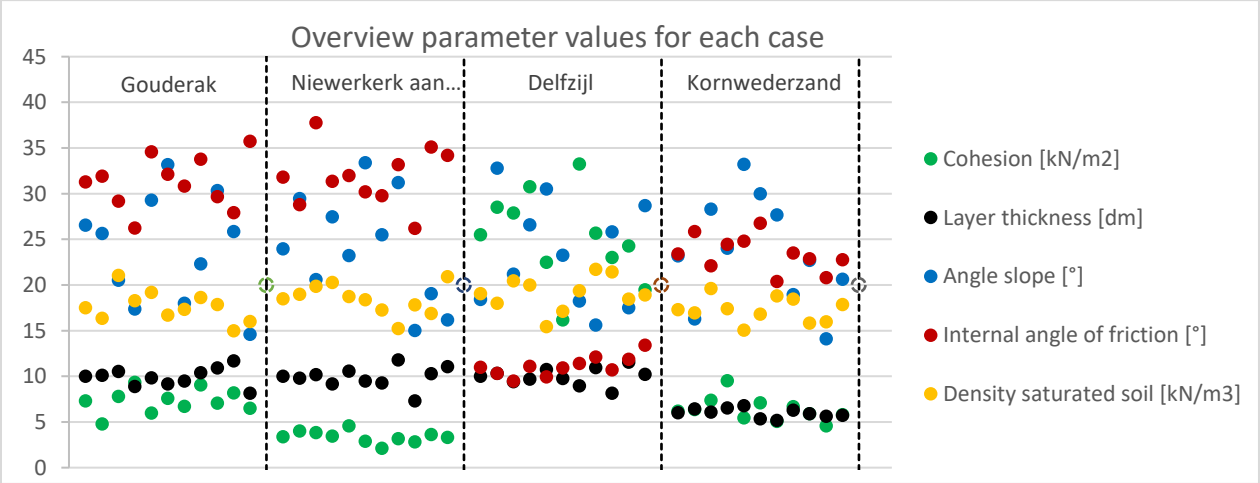

Figure 12 Parameters values for each case, where the first row of parameters in each group is the infiltration experiment followed by the 10 synthetic cases.

The results from the stability assessment of the Spencer-Van der Meij and Edelman & Joustra according to the method described in Sections 3.2.1 and 3.2.2 are plotted as stability factors for all 44 cases in Figure 13. The original case is situated in the middle of the generated cases, except for the stability factor of the Spencer-Van der Meij for the Gouderak case.

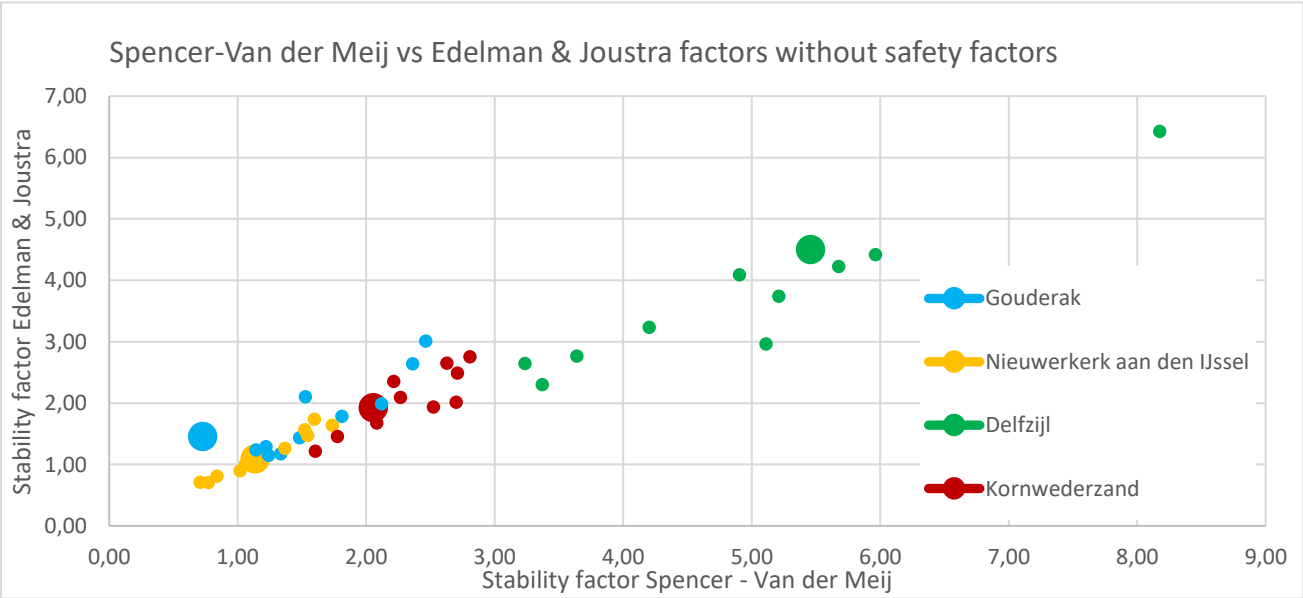

Figure 13 The calculated stability factors for the Spencer-Van der Meij and Edelman & Joustra method are plotted in this figure, where the original case is plotted as a big circle while the synthetic cases are plotted as a dot.

4.1.4 Model parameter Edelman & Joustra

The results from the stability assessment of the Spencer-Van der Meij and Edelman & Joustra in line with the methodology described in Sections 3.2.1 and 3.2.2 are plotted in Figure 14. The stability factors are almost 1:1 for both methods in the lower range, while in the upper range the stability factors for the Spencer-Van der Meij are significantly greater than the stability factor of Edelman & Joustra.

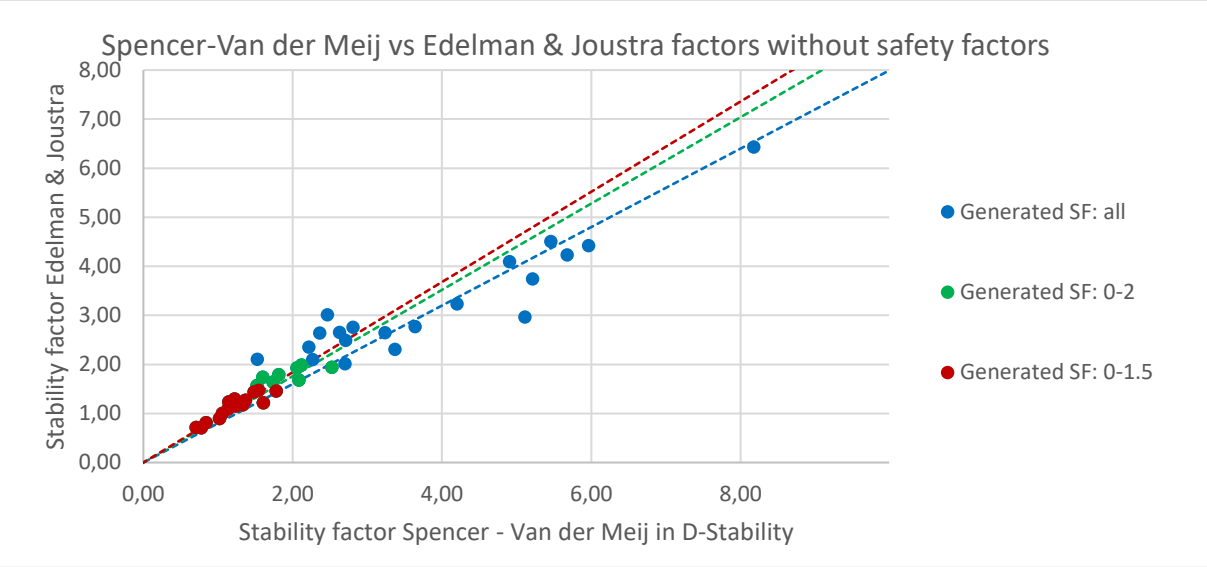

Figure 14 The model parameter of the Edelman & Joustra formula

The results from the methodology described in Section 3.2.3 is presented in Table 4, where the mean and standard deviation are given for the relation between stability factors for Edelman & Joustra and Spencer-Van der Meij.

Table 4 Mean and standard deviation Edelman & Joustra compared with Spencer-Van der Meij

Considered cases	Mean	Standard deviation
Stability factor all	0.800	0.393
Stability factor 0:2	0.913	0.149
Stability factor 0:1.5	0.918	0.111

The results from the methodology described in Section 3.2.3 is presented in Table 5, where the mean and standard deviation of the Edelman & Joustra formula with respect to the Spencer-Van der Meij method has been combined with the mean and standard deviation for the Spencer-Van der Meij from literature.

Table 5 The model parameter of the Edelman & Joustra formula

Combined model parameter	Mean	Standard deviation
Edelman & Joustra and Spencer-Van der Meij	0.963	0.116

4.2Probabilistic assessment

This section addresses the following results:

1. The Target reliability for the mechanism sliding of the landside slope cover.
2. The influence factors for the probabilistic parameters in the Edelman & Joustra formula.
3. The safety-independent factors.
4. The safety-dependent damage factor.
5. Comparing the current- with the new (semi)probabilistic stability assessment.

4.2.2 Determination of the target reliability

The outcome of the determined target reliability is in line with the methodology described in Section 3.3.1. The target reliability is the average value of the safety requirements for sliding of the landside slope cover at the cross-section level for the four infiltration locations, the result of this analysis is presented in Table 6. The value of the target reliability for GABI cover differs from STBI, where target reliability is based on the ultimate limit state from the Eurocode see Table 6 (Kanning, et al., 2016).

Table 6 Target reliabilities for the mechanisms STBI and GABI

Mechanism	**Target reliability [-]**
Macro stability (STBI)	4.3
Sliding of the landside slope cover (GABI)	2.2

4.2.3 Results from the FORM analysis

The influence factors have been determined with the First Order Reliability Method which is described in Section 3.3.2, the results from this analysis are presented in Figure 15. The influence factors for probabilistic parameters, such as cohesion, model, wetted unit weight, layer thickness, and internal angle of friction can range from -1 to 1. A negative value is given to load parameters and positive values to resistance parameters. In Figure 15 the influence factors of the probabilistic parameters are squared and therefore have a positive value between 0 and 1, the sum of the squared influence parameters for each case is always 100%.

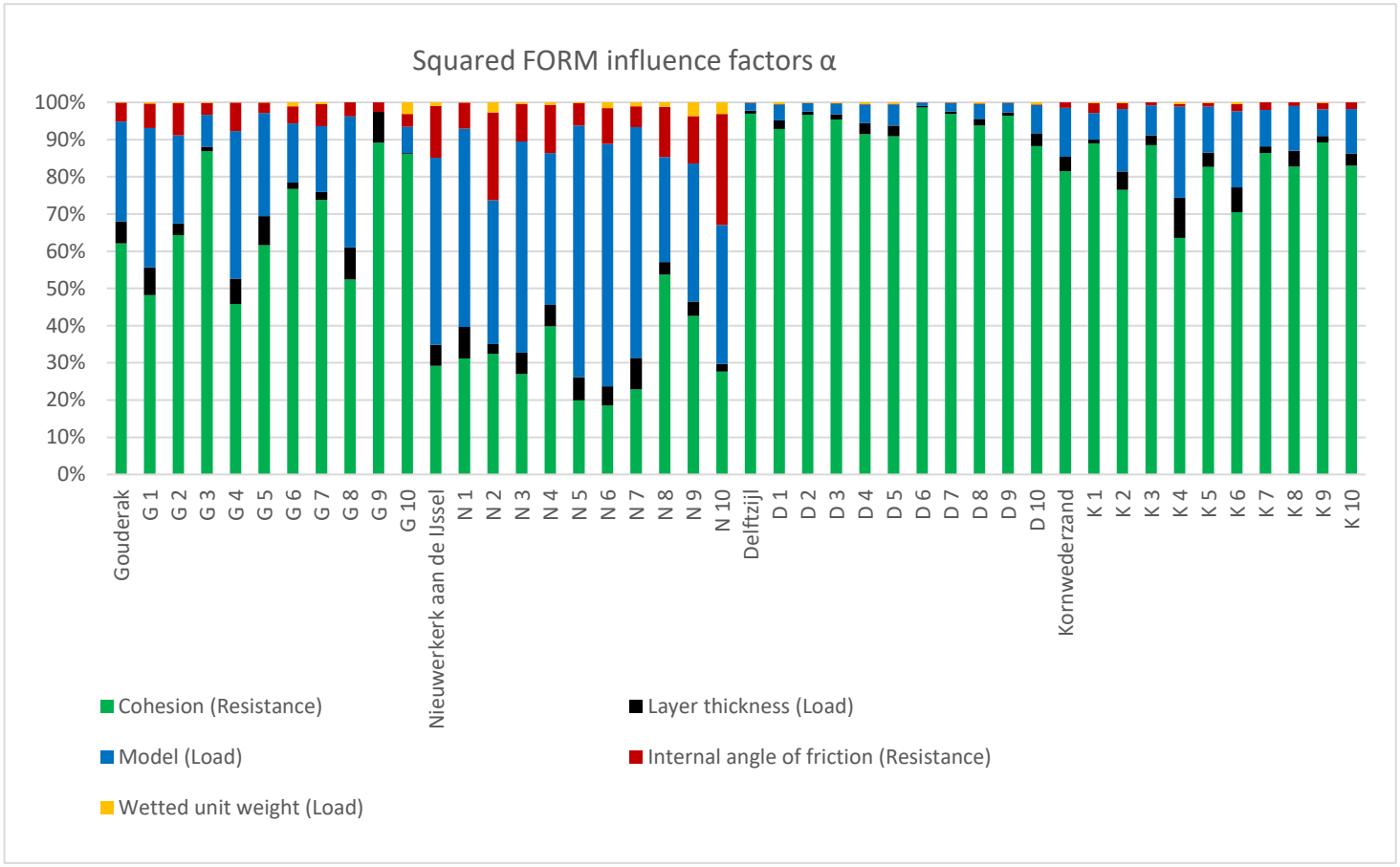

Figure 15 Results from the FORM analysis, where the influence factors are given for each case, where the full name is the original case, and the first letter from the location of the generated synthetic cases.

Safety-in-dependent factors

The safety-in-dependent factors have been determined in line with the methodology described in Section 3.3.2. This results in the following set of the safety in-dependent factors, see Table 7.

Table 7 Safety- in-dependent factors

Y_c	Safety factor cohesion	1.05	[-]
Y_m	Model factor	1.2	[-]
Y_{ϕ}	Safety factor internal angle of friction	1.0	[-]

4.2.4 Calibrating the safety-dependent factor

The safety-dependent partial safety factor has been determined in line with the methodology described in Section 3.3.3. In Figure 16 the relation is shown between the stability factor of Edelman & Joustra with the new safety-in-dependent factors and the reliability index from the probabilistic FORM analysis, an 80% least squared best-fit line is fitted through these points. The semi-probabilistic calibration relation with stability factors ranging from 0-2.5 gives the best results with respect to the probabilistic assessment as can be seen in Appendix G and H.

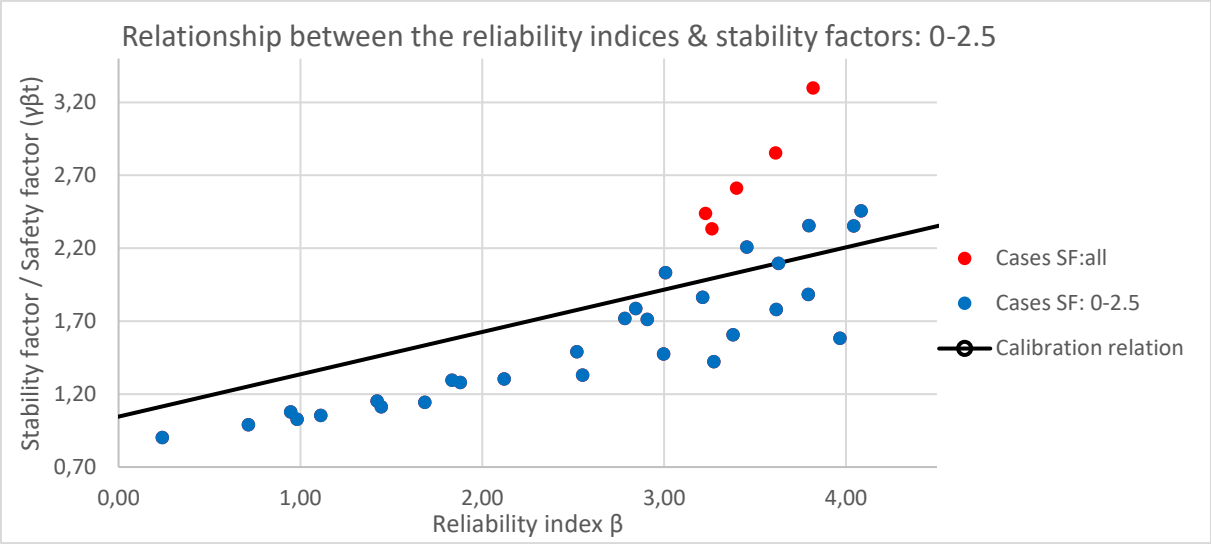

Figure 16 Calibration of the safety dependent partial safety factor, for stability factors between 0-2.5, expressed in blue and the total cases expressed in blue and red.

This results in the following safety-dependent damage factor:

$$Y_n : 0.29 \cdot \beta_T + 1.05$$

Where:

β_T is the safety requirement for the cross-section for the mechanism sliding of the landside slope cover, see Equation 4.

4.2.5 The optimal safety factors for Edelman & Joustra

An overview is given of the new safety factors from Sections 4.2.3 and 4.2.4 and the current safety factors from Section 2.1.2, see Table 8.

Table 8 current and new partial safety factors Edelman & Joustra

Current safety factors

$Y_{m,\emptyset}$	Partial safety factor tangent Ø	1.1	[-]
$Y_{m,c}$	Partial safety factor *c*	1.25	[-]
Y_m	Model factor	1.1	[-]
Y_n	Damage factor	1.1	[-]

New safety factors

$Y_{m,\emptyset}$	Partial safety factor tangent Ø	1.0	[-]
$Y_{m,c}$	Partial safety factor *c*	1.05	[-]
Y_m	Model factor	1.2	[-]
Y_n	Damage factor	$0.29 \cdot \beta_T^* + 1.05$	[-]

$^*\beta_T$ is the safety requirement for the cross-section for the mechanism sliding of the landside slope cover, which can be calculated with Equation 4.

4.2.6 Comparing the current- and the new stability assessment

The new (semi) probabilistic method is compared to the current method by assessing the stability factor of the 44 cases, see Figure 17. The new method takes into account the exceedance probability of an overtopping discharge of 1.0 l/s/m, the length effect, the trajectory norm, and the failure budget, whereas the current method does not take into account these factors.

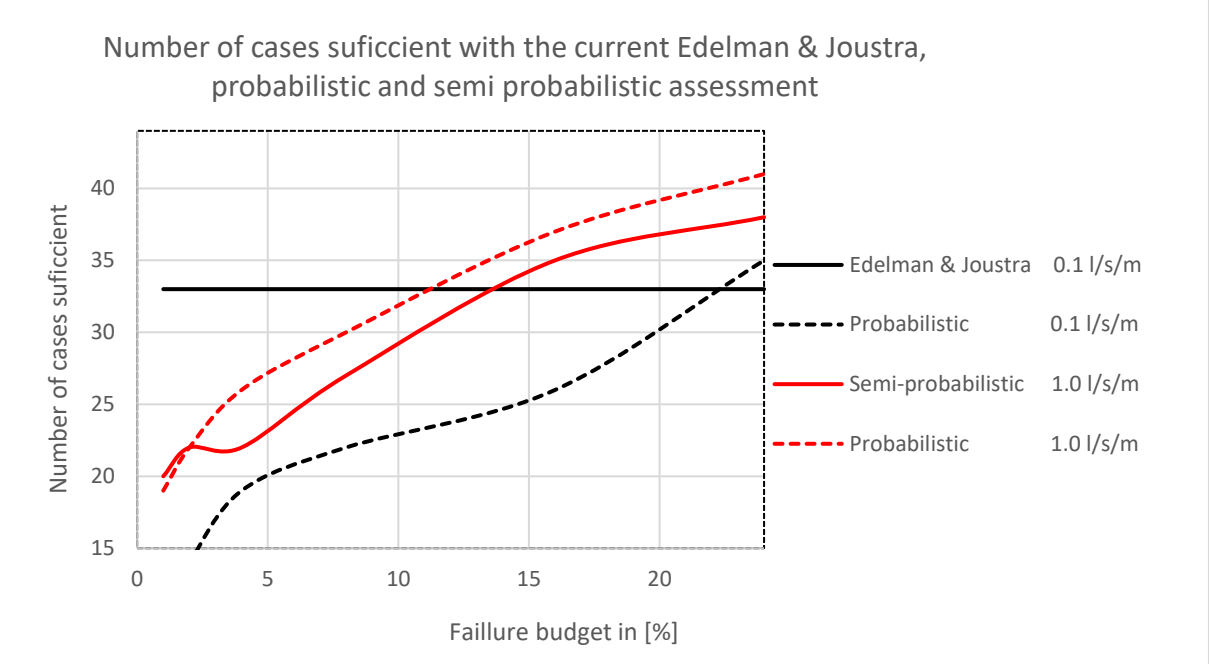

Figure 17 Outcome of the current-, the semi-probabilistic and the probabilistic assessment as a function of the failure budget

In Figure 18 the results of the current- and the new stability assessment of the Edelman & Joustra method are compared. The stability assessment for cases with a gradient of 1V:4H and 1V:3H are all stable according to the current- and the new stability method.

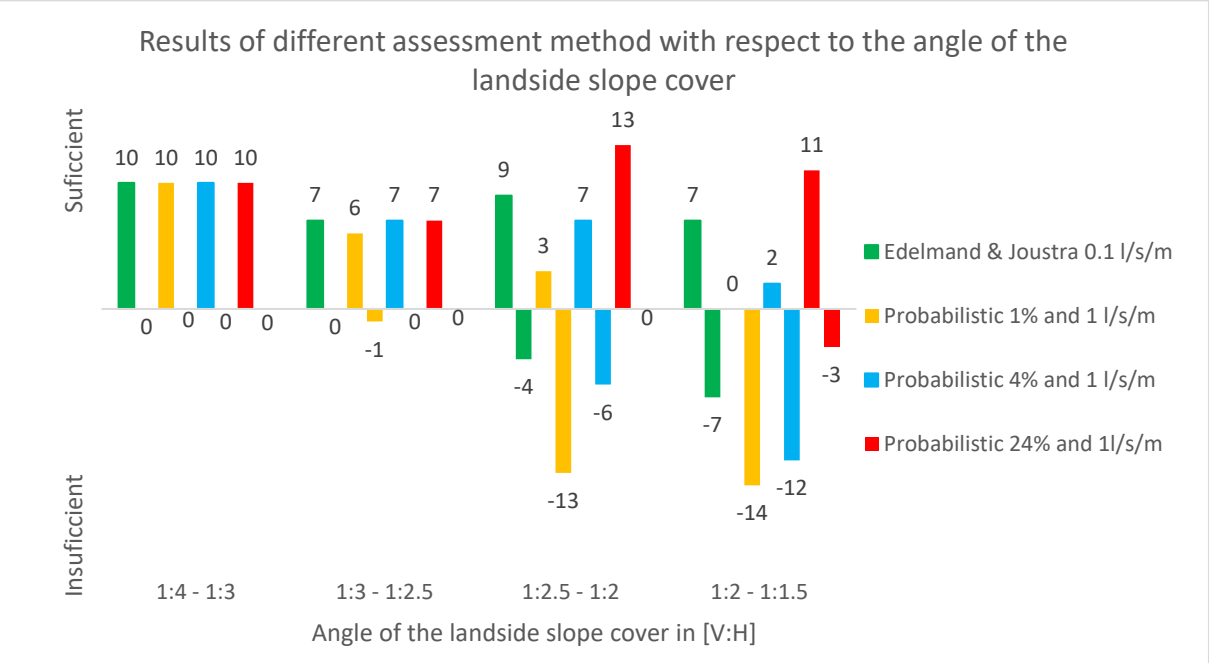

Figure 18 Stability assessment with the current Edelman & Joustra and the probabilistic assessment in combination with the safety requirement for different failure budgets.

5. Discussion

The aim of this research is to evaluate whether optimization of the partial safety factors in the Edelman & Joustra formula is possible and to develop a semi-probabilistic approach to assess the stability of the landside slope cover for clay flood embankments in the Netherlands.

The Spencer-Van der Meij method in D-stability is able to reproduce all experimental outcomes from the infiltration tests, see Figure 11. The Edelman & Joustra formula is only able to reproduce the experimental outcomes correctly for cases that consist of a homogeneous clay profile, which is in line with (Rijkswaterstaat, 2021). Therefore, the probabilistic analysis only considers the original- and synthetic cases that consist or behave as pure clay flood embankments. Incorporating the unstable case would lead to an outlier in the data set and increase the uncertainty, which leads to a lower target reliability index and results in a stricter assessment.

The model parameters, the mean and standard deviation for the Edelman & Joustra formula with a stability factor from 0 to 1.5 are chosen to determine the model uncertainty, see Table 5. These stability factors indicate situations that are close to being stable or unstable. This results in a higher safety factor for the model, as the current method see Table 8. Considering larger stability factors would lead to more uncertainty and therefore a lower target reliability index which results in a stricter assessment.

The dataset consists of four infiltration experiments, for each experiment, 10 synthetic cases were generated. The synthetic cases for one location share the same outer slope geometry. This results in the same exceedance probability of the overtopping discharge for the infiltration case as for the 10 synthetic cases. This also holds for the other case-specific parameters as, the trajectory norms, failure budget and length effect. The optimal safety factors are determined with a target reliability of 2.2 this is the average safety requirement for all 44 cases, see Table 6. Therefore too few locations are considered representative for all primary clay flood embankments in the Netherlands. The chosen target reliability gives better results than the target reliability from the Eurocode, which leads to unrealistic values for the parameter of cohesion. Adding more cases with cross-sectional safety requirements, could lead to different safety-independent factors, however this is will be compensated by the safety-dependent factor which is determined by the calibration relation.

The calibration relation is shown in Figure 16, compared to the calibration relation of macro stability the target reliability indices are significant lower (Kanning, et al., 2016). This is because sliding of the landside slope cover only occurs when the cover layer is complete saturated. Adding more synthetic cases or removing cases does not affect the calibration relation itself. Adding more cases with location-specific parameters can have a minor effect on the calibration relation, because the target reliability changes the safety-independent factors.

While the current stability assessment with Edelman & Joustra is often considered conservative, the results show that this method is rather optimistic, see Figure 17. This optimism is the result of not including the length effect, trajectory norms, and the exceedance probability of the overtopping discharge.

In the new stability assessment, the overtopping discharge of 1.0 l/s/m was chosen. An overtopping discharge of 0.1 l/s/m would result in a strict approach as can be seen from Figure 17. An overtopping discharge of 0.1 l/s/m does not lead to a parallel groundwater flow, where 1.0 l/s/m does (Van Hoven, et al., 2010). The amount of water that can infiltrate is highly dependent on the discharge over time and the type of wave overtopping, therefore other criterion, than a certain discharge value should be considered.

Currently, there is no fixed failure budget reserved for sliding of the landside slope cover. The effect of the failure budget on the stability assessment is displayed in Figure 17. Flood embankment managers are free to distribute the available failure budget between the different failure mechanisms in the custom assessment. However, this does not occur in current practice, because it is too cumbersome to optimize the failure budget for each mechanism and cross-section for a certain trajectory. This is unfortunate because the strength of the failure probability approach is not used to its full potential.

6. Conclusions and recommendations

In this study the following research question is answered: '' How can the stability assessment of the Edelman & Joustra formula be optimized for clay flood embankments in the Netherlands within the legal assessment instrument?'' A probabilistic calibration study was performed to determine the optimal partial safety factors for the Edelman & Joustra formula. The current stability assessment of the landside slope cover due to wave overtopping on clay flood embankments has been improved by incorporating a safety-dependent damage factor in the Edelman & Joustra formula. This factor takes into account the length effect, the trajectory norms, the failure budget, and the exceedance probability of the overtopping discharge. The newly derived safety factors prevent unnecessary rejection and over dimensioning of flood embankments so the available resources for flood embankment improvements can be used better.

To improve the stability assessment of the landside slope cover even further, the following research subject is recommended . In the current assessment, an overtopping discharge is considered. However, the amount of water that can infiltrate is highly dependent on the discharge over time and the type of wave overtopping. Therefore other criterion, than a certain discharge value should be included in the safety requirement.

Bibliography

Akkerman, G., Van Gerven, K., & Schaap, H. (2007). *Wave overtopping erosion tests at Groningen sea dyke.* Royal Haskoning and Infram.

Baarse, P., & de Grave, G. (2011). *Kosten van maatregelen informatie ten behoeve van het project waterveiligheid 21e eeuw.* Delft: Deltares.

De Visser, M., & Jongejan, R. (2018). *KPR Factsheet werkwijze macrostabiliteit i.c.m. golfoverslag.*

Deltares. (2010). *SWB Golfoverslag en sterkte dijk bekleding, 3D evaluatie Afsluitdijk.* Delft: Deltares.

Javankhoshdel, S. (2019, 6 21). *Which is the best LEM method for determination of Slope Stability*. Retrieved from Researchgate: https://www.researchgate.net/post/Which-is-the-best-LEM-method-for-determination-of-Slope-Stability

Jongejan, R. (2017). *WBI 2017 Code calibration.* Rijkswaterstaat.

Jonkman, S., Steenbergen, R., Morales-Napoles, O., Vrouwenvelder, A., & Vrijling, J. (2017). *Probabilistic design: Risk and reliability analysis in Civil Engineering.* Delft: TU Delft.

Kanning, W., Teixeira, A., Van der Krogt, M., & Rippi, K. (2016). *Calibration STBI 2016.* Delft: Deltaris.

Kok, M., & Jongejan, R. (2016). *Fundementals of flood protection.* RWS en ENW.

Mai, C., Van Gelder, P., & Vrijling, J. (2006). *Safety of coastal defences and flood risk analysis.* London: Taylor and francis group.

NEN, Nederlands normalisatie-instituut. (2012). *NEN 9997-1+1C 2012 Geotechnisch ontwerp van constructies.* Delft.

Noordam, A., & Van Hoven, A. (2018). *POVM Infiltratieproef II Analyse Infiltratieproef IJsseldijk.* POV macrostabiliteit.

NOS. (n.d.). *Watersnood: een reconstructie van de watersnoodramp in 1953*. Retrieved from nos: https://lab.nos.nl/projects/watersnood/index.html

Rijkswaterstaat. (1961). *Verslag over de stormvloed van 1953.* Den Haag: Staatsdrukkerij en uitgeverijbedrijf.

Rijkswaterstaat. (2021). *Schematiseringhandleiding grasbekleding WBI 2017.* Rijkswaterstaat.

SH piping. (2019). *Schematiseringhandleiding piping.* Utrecht: Ministerie van Infrastructuur en Water.

't Hart, R. (2018). *Fenomenologische beschrijving WBI.* Delft: Delteres.

TAW. (1996). *Technisch rapport klei voor dijken.* Rijkswaterstaat.

TAW. (2001). *Addendum bij het technisch rapport waterkerende grondconstructies.* Rijkswaterstaat.

TAW. (2001). *Technisch rapport waterkerende grondconstructies: geotechnische aspecten van dijken, dammen en boezemkaden.* Rijkswaterstaat.

TAW. (2004). *Technisch rapport waterspanningen bij dijken.* Rijkswaterstaat.

Van Damme, M., Hulst, M., Bottema, M., Van Hemert, H., Heerema, J., & Stenveld, L. (2021, 4). Discussie n.a.v. presentatie tijdens de team techniek special: afstuderen Lars Stenveld GABI. Den Haag, Zuid Holland, Nederland: Rijkswaterstaat.

van Deen, J., de Bruijn, H., & Van Duinen, A. (2019). *Schematiseringshandleiding macrostabiliteit WBI 2017.* Rijkswaterstaat.

Van der Meer, J. (2008). *Erosion strength of inner slopes of dikes: preliminary conclusions after two years of testing.* Akkrum.

Van der Meer, J., Verheij, H., Lindenberg, J., & Van Hoven, A. (2007). *Golfoverslag en sterkte binnentaluds van dijken Rapport predictiespoor SBW.* Infram & Deltares.

Van der Ruyt, M. (2018). *POVM infiltratieproef II: Factual raport infiltratieproef II langs de Groenendijk te Nieuwerkerk aan den IJssel.* POV Macrostabiliteit.

Van Duinen, A. (2017). *Modelonzekerheden Spencer-Van der Meij model.* Delft: Deltares.

Van Hoven, A. (2016). *Theorie beoordeling grasbekledingen.* Delft: Deltares.

Van Hoven, A. (2017). *POVM Beter benutten actuele sterkte KIJK: factual raport infiltratieproef IJsseldijk.* POV Macrostabiliteit.

Van Hoven, A. (2019). *Schematiseringshandleiding microstabiliteit WBI 2017.* Rijkswaterstaat.

Van Hoven, A., Hardeman, B., Van der Meer, J., & Steendam, J. (2010). *Sliding stability of landward slope clay cover layers of sea dikes subject to wave overtopping.*

Verheij, H., Hofmans, G., Steendam, G., Van der Meer, J., & Van Hoven, A. (2010). *SBW golfoverslag en sterkte grasbekledingen: Fase 3D evaluatie Afsluitdijk.* Delft: Deltares.

Waterschappen, Rijkswaterstaat, Deltares, & Ingenieursbureaus. (2021). KKP: grasbekledingen. (L. Stenveld, Interviewer)

Appendix

A. Stability calculation

The stability of the landside slope cover is calculated in the program D-stability which is used in the WBI. The stability calculation is manually performed for all 44 cases.

1. **The geometry of the cross-section:** of the flood embankment is modelled. For 43 cases this consists of a pure clay flood embankment. Only the unstable case of Gouderak consisted of a small sand layer between the clay core and cover layer, this is also schematized. The cover layer is modelled as a separate layer as the core, both layers having the same strength parameters, this has no effect on the outcome, but the slip planes are easier to define see Step 4, see Figure 19.

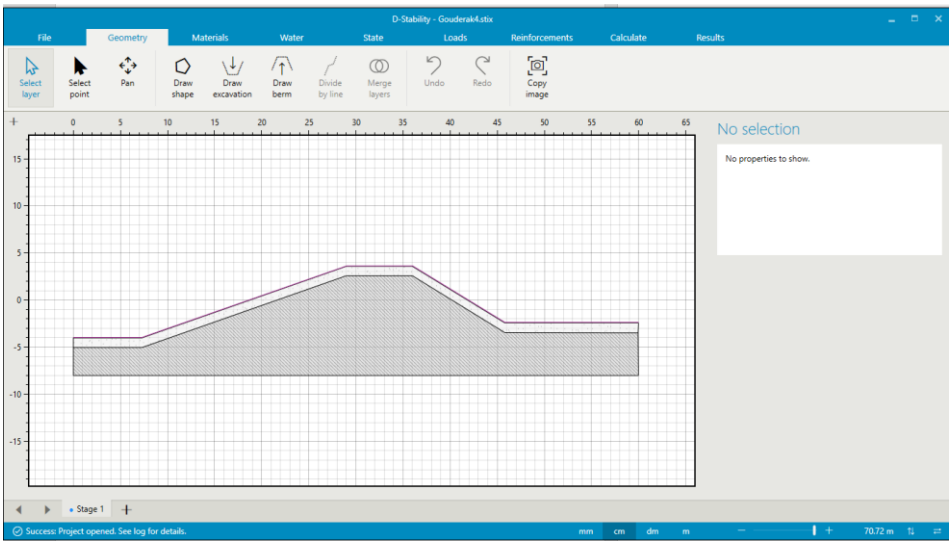

Figure 19 D-Stability geometry

1. **Materials:** within the mechanism sliding of the landside slope cover the drained Mohr-Coulomb parameters are applied, see Figure 20 (Van Hoven, 2016). The parameters are the deterministic values.

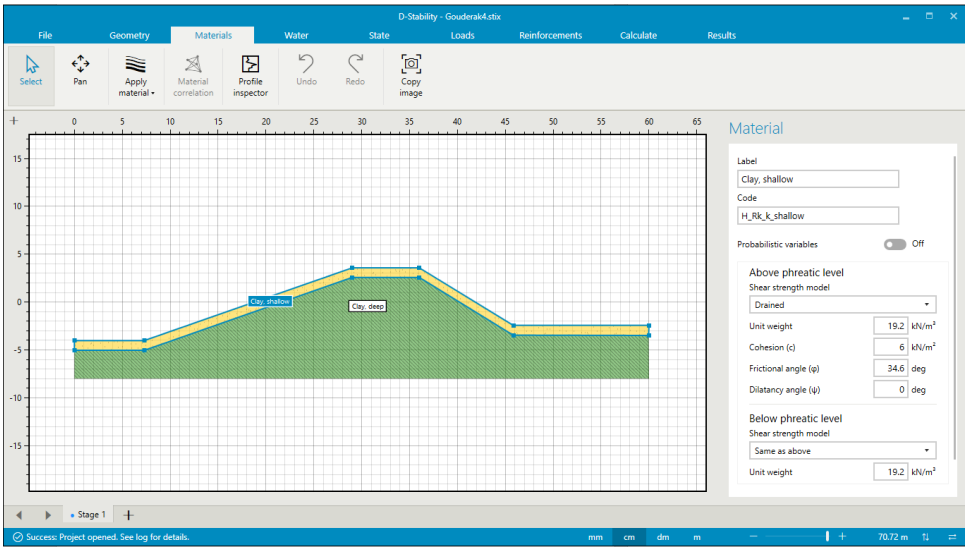

Figure 20 D-Stability materials

2. **Phreatic level**: according to the WBI the phreatic level has to be modelled on the landside slope cover to simulate a saturated cover layer, see Figure 21 (Rijkswaterstaat, 2021).

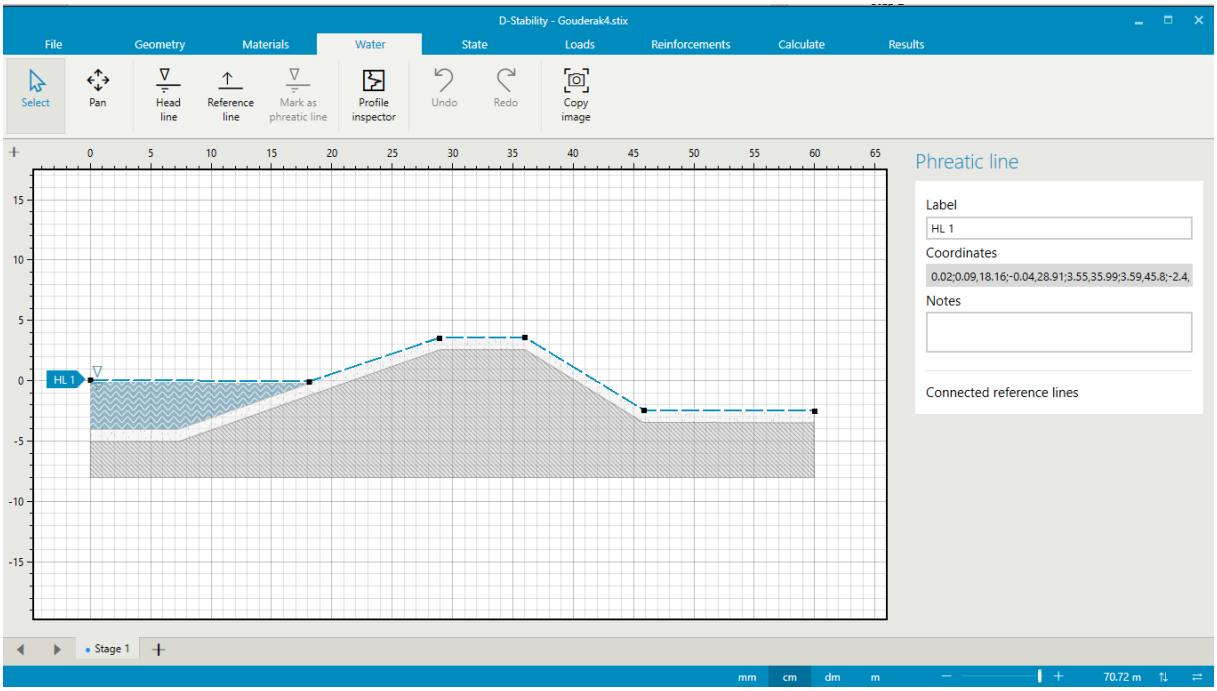

Figure 21 D-Stability phreatic level

3. **Reinforcements**: for the control calculations with the Bishop method, a forbidden line is schematized to restrict the critical slip plane to the cover layer, see Figure 22.

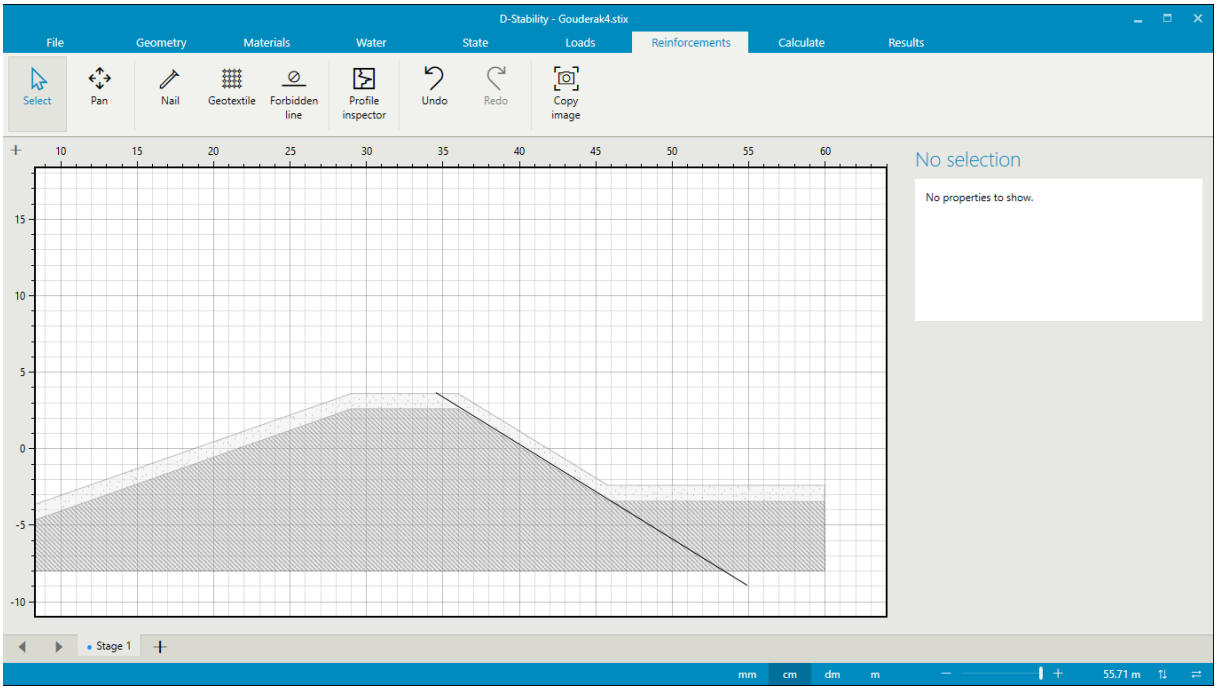

Figure 22 D-stability reinforcements

4. **Calculations**: The stability factor is calculated for the Spencer-Van der Meij and the Bishop. For both methods, a search method is used to find the most critical slip plane, see Figure 23 and Figure 24.

Spencer-Van der Meij

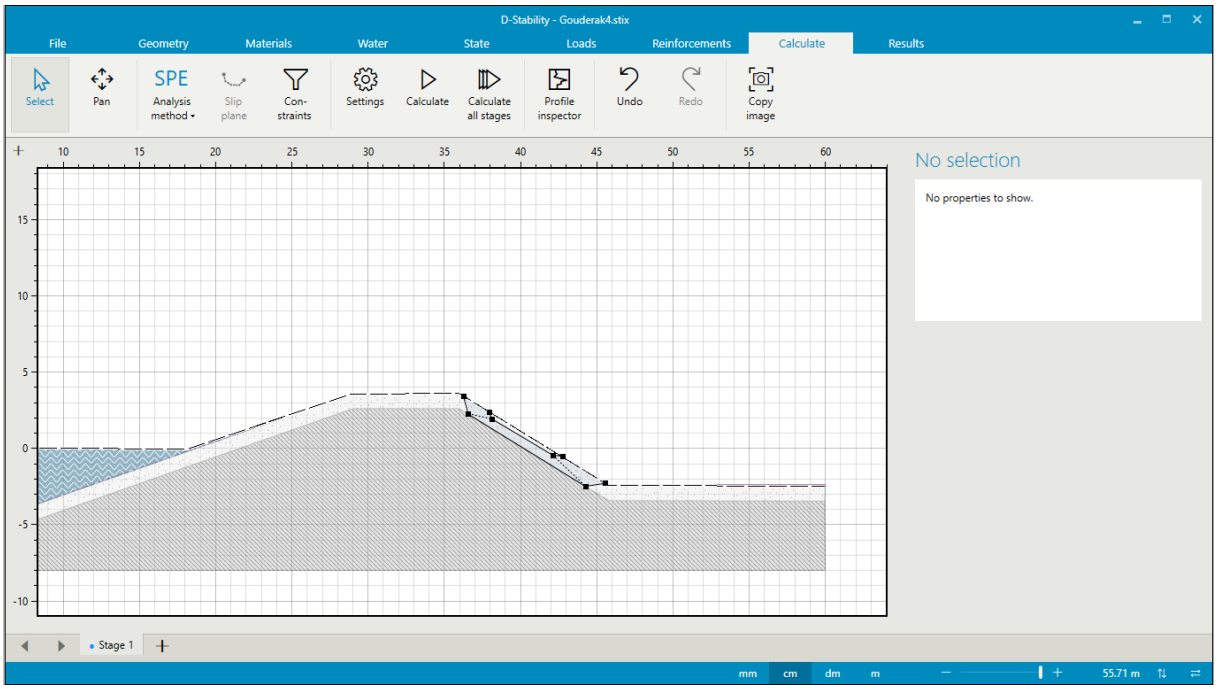

Figure 23 D-stability Spencer-Van der Meij calculations

Bishop

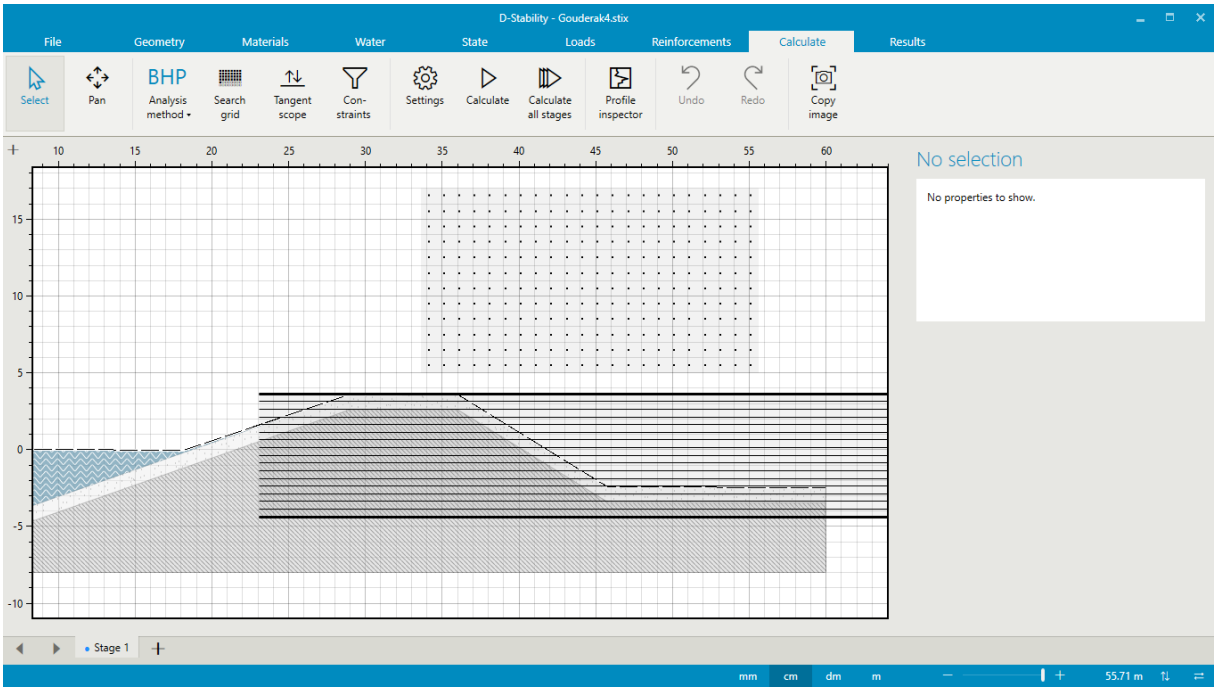

Figure 24 D-stability Bishop calculation

5. **Results**: for both methods the calculated stability factor are given, see Figure 25 and Figure 26.

Spencer-Van der Meij

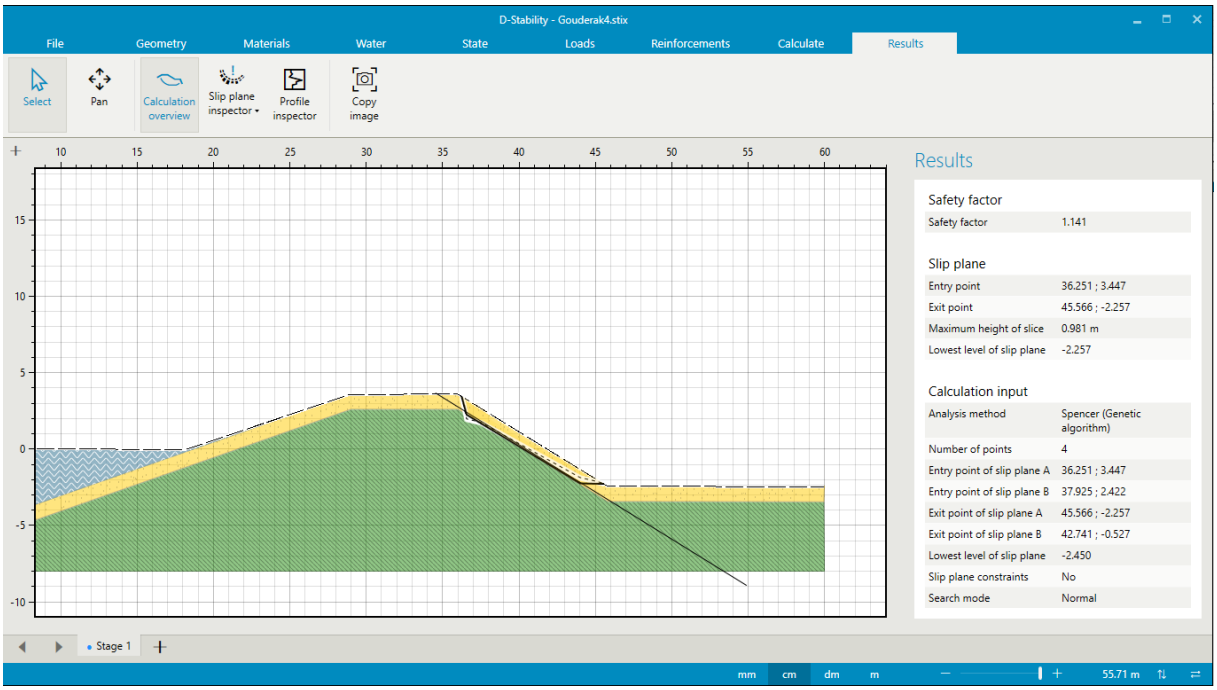

Figure 25 D-stability Spencer-Van der Meij results

Bishop

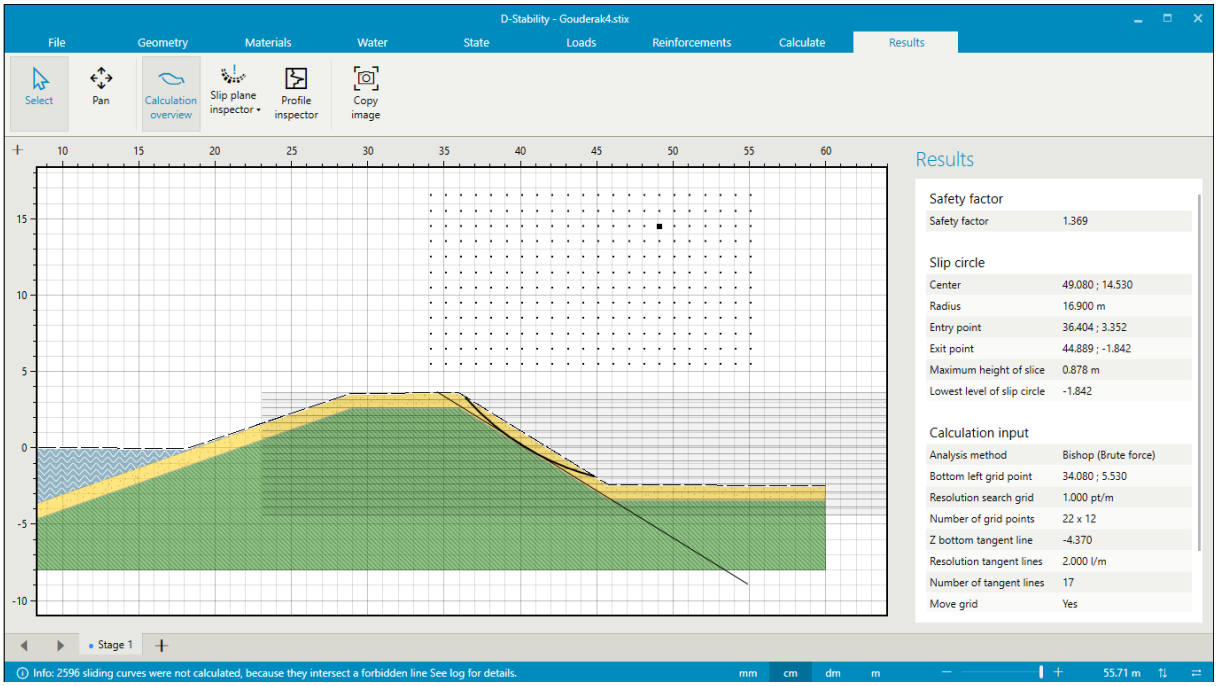

Figure 26 D-Stability Bishop results

B. Dataset

The code for the Latin Hypercube sampling for one case is given in Figure 27, this step is repeated for the three other infiltration cases.

```
clear clc, close all;

%variables sampling
% N: number of samples 10, for each case
N=10;
% P: number of variables 5
P=5;
%generating the latin hypercube matrix 10 samples (rows) by 5 variables
%(colum)
x=lhsdesign(N,P);

%variables aanpasbaar mu alleen

%1D=layer thickness, normal dist
mud=0.6;  sigd= 0.1*mud; xd=x(:,1);
d=icdf('normal',xd,mud,sigd);
d=d';

%2A= angel of land side slope cover, uniform dist
%from 1:1,5 to 1:4
mua1=33.69; mua2=14;04; xa=x(:,2);
a=xa*(mua1-mua2)+mua2;
a=a';

%3I= internal angle of friction, normal dist
mui=23.4; sigi= 0.1*mui; xi=x(:,3);
i=icdf('normal',xi,mui,sigi);
i=i';

%4C= cohesion, normal dist
muc=6.2; sigc=0.2*muc; xc=x(:,4);
c=icdf('normal',xc,muc,sigc);
c=c';

%5P= saturated unit weight
mup=17.3;  sigp=0.1*mup; xp=x(:,5);
p=icdf('normal',xp,mup,sigp);
p=p';

data_processed=([d;a;i;c;p]);
csvwrite('file.csv',data_processed)
```

Figure 27 MATLAB Latin Hypercube sampling script

The results of the generation of the dataset with the Latin Hypercube sampling method for each location are presented in Table 9, Table 10, Table 11, and Table 12.

Delfzijl

Table 9 Dataset Delfzijl

Parameters		Delfzijl original	Delf 1	Delf 2	Delf 3	Delf 4	Delf 5	Delf 6	Delf 7	Delf 8	Delf 9	Delf 10
Layer thickness	[m]	1,0	1,0	0,9	1,0	1,1	1,0	0,9	1,1	0,8	1,2	1,0
Land side slope cover H:V	[-]	0,3										
Land side slope cover	[°]	18,4	32,8	21,2	26,6	30,5	23,2	18,3	15,6	25,8	17,5	28,7
Internal angle of friction	[°]	11,0	10,3	9,5	11,1	10,0	10,9	11,4	12,1	10,7	11,9	13,4
Cohesion	[kN/m2]	25,5	28,5	27,9	30,8	22,5	16,2	33,3	25,7	23,0	24,3	19,5
Density saturated soil	[kN/m3]	19,1	18,0	20,5	20,0	15,5	17,1	19,4	21,7	21,4	18,5	18,9
Density water	[kN/m3]	10,3	10,0	10,0	10,0	10,0	10,0	10,0	10,0	10,0	10,0	10,0
Lenght slope		16,0	10,0	14,9	12,1	10,6	13,7	17,2	20,0	12,4	17,9	11,2

Kornwederzand

Table 10 Dataset Kornwederzand

Parameters		Korn original	Korn 1	Korn 2	Korn 3	Korn 4	Korn 5	Korn 6	Korn 7	Korn 8	Korn 9	Korn 10
Layer thickness	[m]	0,6	0,6	0,6	0,7	0,7	0,5	0,5	0,6	0,6	0,6	0,6
Land side slope cover H:V	[-]	0,4										
Land side slope cover	[°]	23,2	16,3	28,3	24,0	33,2	30,0	27,7	18,9	22,7	14,1	20,6
Internal angle of friction	[°]	23,4	25,9	22,1	24,4	24,8	26,8	20,4	23,5	22,9	20,8	22,8
Cohesion	[kN/m2]	6,2	6,4	7,4	9,5	5,5	7,1	5,1	6,7	5,9	4,6	5,8
Density saturated soil	[kN/m3]	17,3	16,9	19,6	17,4	15,1	16,8	18,8	18,5	15,8	16,0	17,9
Density water	[kN/m3]	10,3	10,0	10,0	10,0	10,0	10,0	10,0	10,0	10,0	10,0	10,0
Lenght slope		7,9	10,7	6,3	7,4	5,5	6,0	6,5	9,2	7,8	12,3	8,5

Gouderak

Table 11 Dataset Gouderak

Parameters		Goud orginal	Goud 1	Goud 2	Goud 3	Goud 4	Goud 5	Goud 6	Goud 7	Goud 8	Goud 9	Goud 10
Layer thickness	[m]	1,0	1,0	1,1	0,9	1,0	0,9	0,9	1,0	1,1	1,2	0,8
Land side slope cover H:V	[-]	0,5										
Land side slope cover	[°]	26,6	25,6	20,5	17,4	29,3	33,2	18,0	22,3	30,3	25,8	14,6
Internal angle of friction	[°]	31,3	31,9	29,2	26,2	34,6	32,1	30,8	33,8	29,7	27,9	35,8
Cohesion	[kN/m2]	7,3	4,8	7,8	9,3	6,0	7,6	6,7	9,1	7,1	8,2	6,5
Density saturated soil	[kN/m3]	17,5	16,4	21,0	18,3	19,2	16,7	17,3	18,6	17,9	15,0	16,0
Density water	[kN/m3]	10,0	10,0	10,0	10,0	10,0	10,0	10,0	10,0	10,0	10,0	10,0
Lenght slope		14,4	12,7	15,7	18,4	11,2	10,0	17,8	14,5	10,9	12,6	21,8

Niewerkerk aan den IJssel

Table 12 Dataset Niewerkerk aan den IJssel

Parameters		Niew orginal	Nieuw 1	Nieuw 2	Nieuw 3	Nieuw 4	Nieuw 5	Nieuw 6	Nieuw 7	Nieuw 8	Nieuw 9	Nieuw 10
Layer thickness	[m]	1,0	1,0	1,0	0,9	1,1	0,9	0,9	1,2	0,7	1,0	1,1
Land side slope cover H:V	[-]	0,4										
Land side slope cover	[°]	24,0	29,5	20,6	27,5	23,2	33,4	25,5	31,2	15,0	19,1	16,2
Internal angle of friction	[°]	31,8	28,8	37,8	31,3	32,0	30,2	29,8	33,2	26,2	35,1	34,2
Cohesion	[kN/m2]	3,4	4,0	3,9	3,4	4,6	2,9	2,1	3,2	2,8	3,6	3,3
Density saturated soil	[kN/m3]	18,5	19,0	19,8	20,3	18,7	18,4	17,3	15,2	17,8	16,9	20,9
Density water	[kN/m3]	10,0	10,0	10,0	10,0	10,0	10,0	10,0	10,0	10,0	10,0	10,0
Lenght slope		9,4	8,1	11,4	8,7	10,1	7,3	9,3	7,7	15,4	12,2	14,4

C. Exceedance probability critical overtopping discharge

The exceedance probability is calculated in the program Hydra-NL which is the recommended software in the WBI. The analysis is step-by-step described in the following section. The calculation is performed for, Kornwederzand, Delfzijl, Gouderak and Niewerkerk aan den IJssel.

1. Selecting the location of the experiment, in Figure 28 the location of the infiltration test on the Afsluitdijk near Kornwederzand is selected.

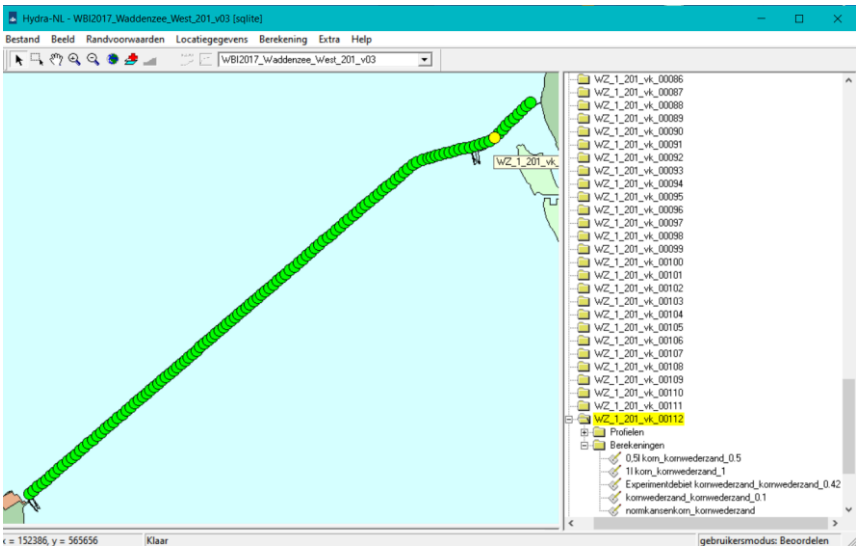

Figure 28 Hydra-NL location cross-section

2. In Figure 29 the geometry of the seaward side of the flood embankment for the location Kornwederzand is schematized and the direction of the flood embankment with respect to the North.

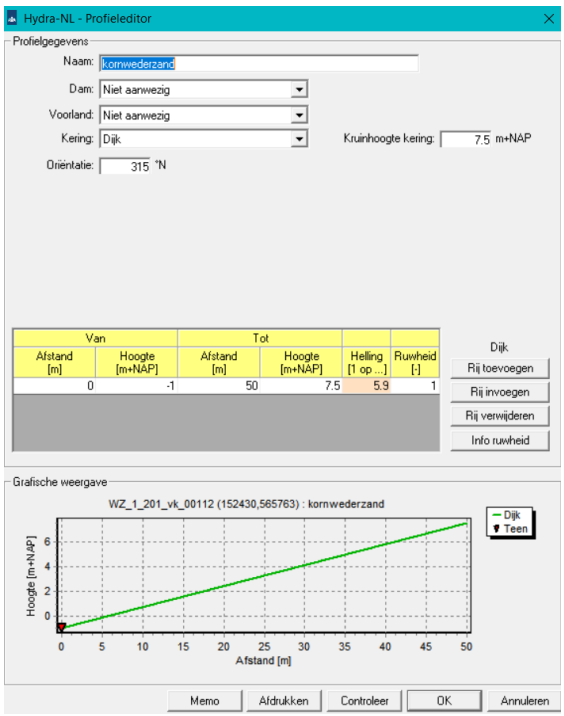

Figure 29 Hydra-NL geometry of the seaside slope cover

3. In Figure 30 the critical overtopping discharge of 1.0 l/s/m is defined.

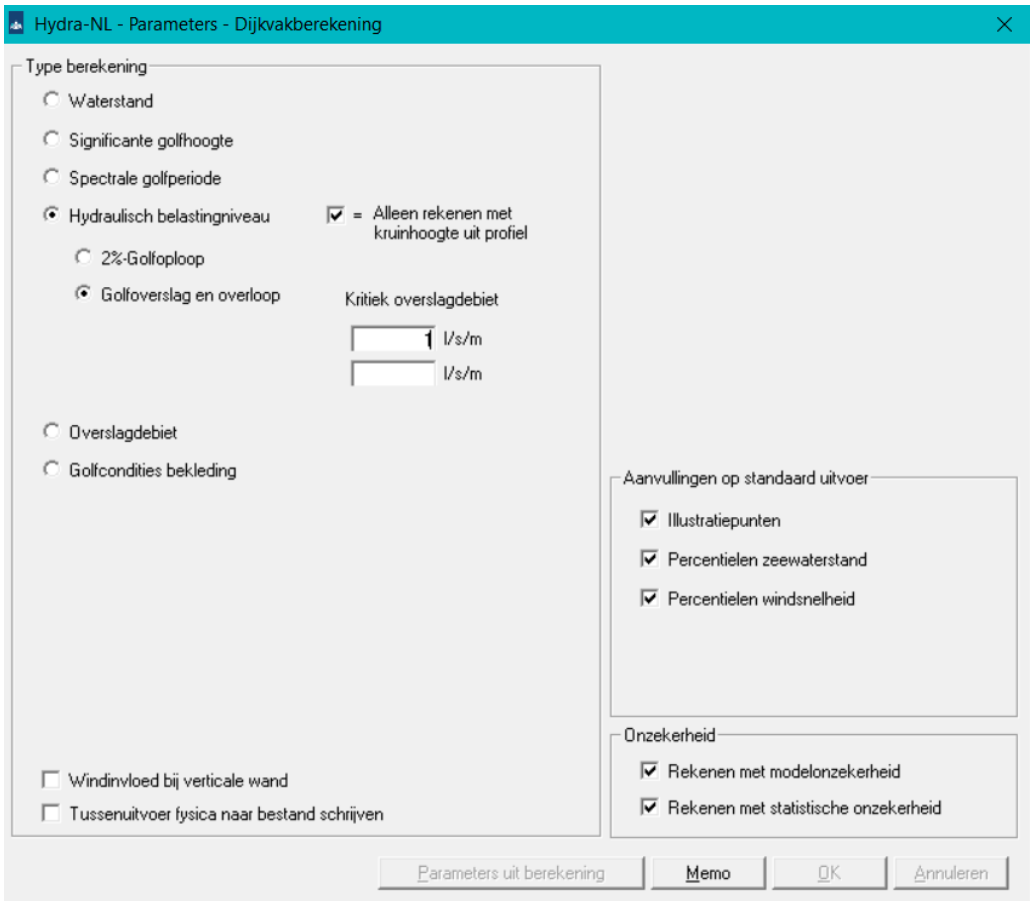

Figure 30 Hydra-NL parameters calculation

4. The previous steps lead to the following results for the location Kornwederzand as can be seen in Figure 31.

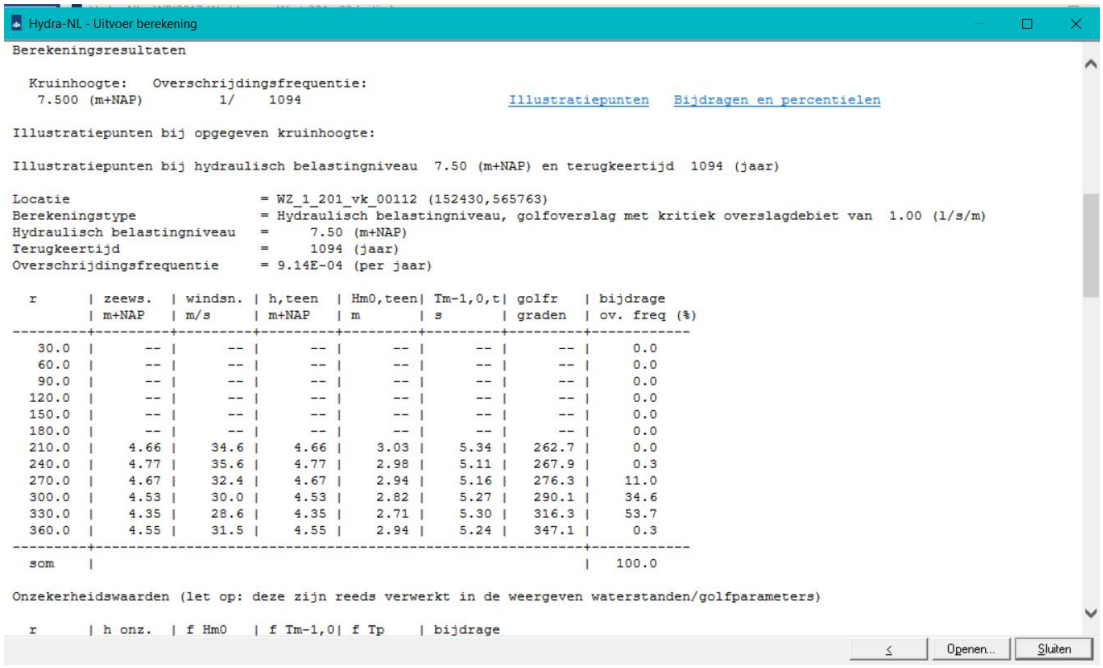

Figure 31 Hydra-NL results

D. FORM calculation

The FORM analysis is performed in the program Prob2b. The analysis is step-by-step described in the following section.

1. In Figure 32 the parameters are defined with the mean being the generated- or measured values from infiltration experiment and the standard deviation and their distribution according to the WBI and (NEN, 2012)

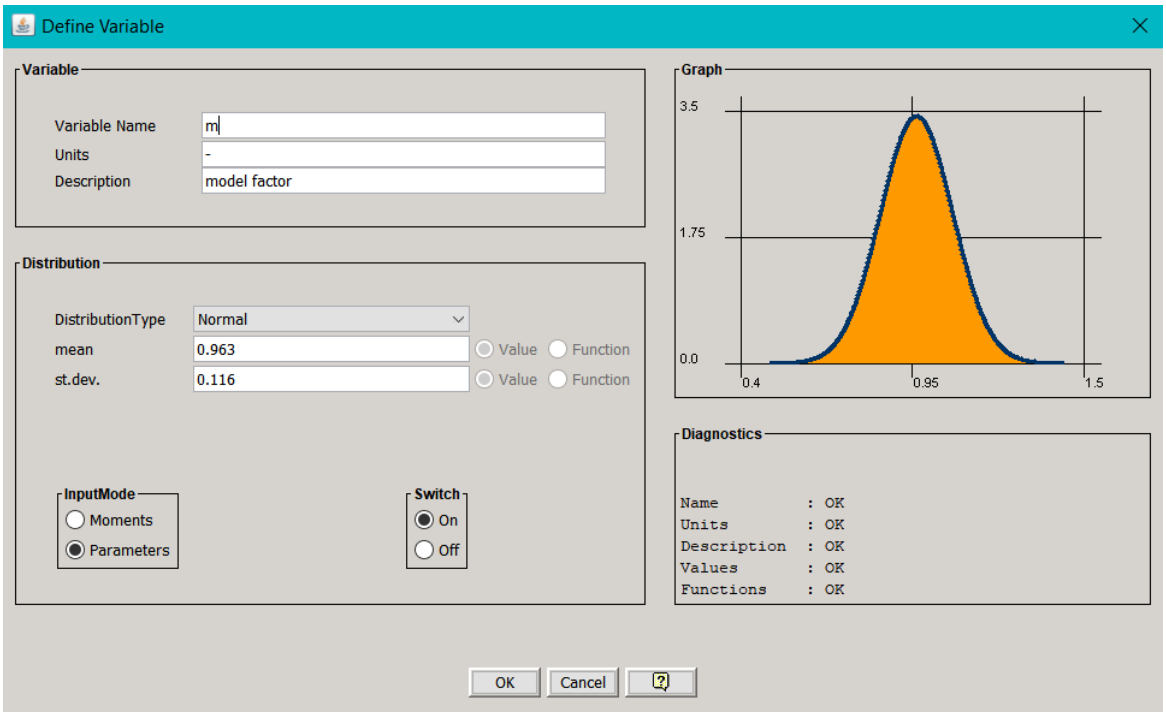

Figure 32 Prob2B defining the parameters

2. An overview of the parameters in the Edelman & Joustra formula is given in Figure 33.

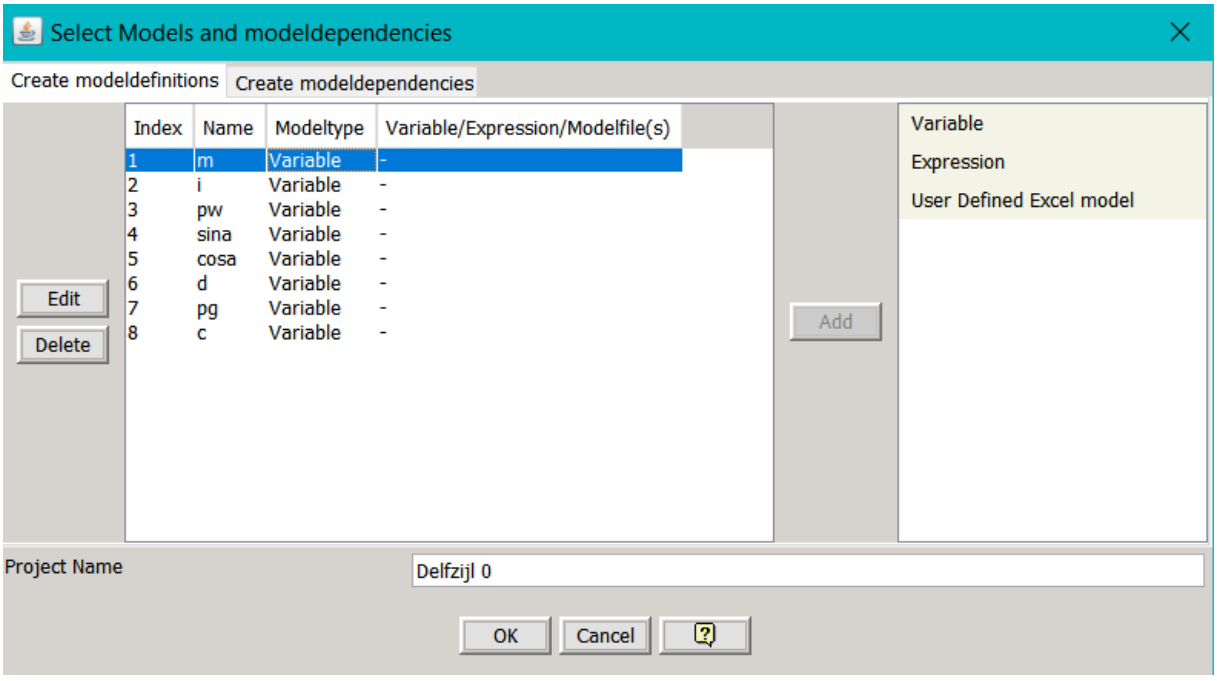

Figure 33 Prob2B overview of the parameters

3. The Z-function of the Edelman & Joustra formula is defined in Figure 34.

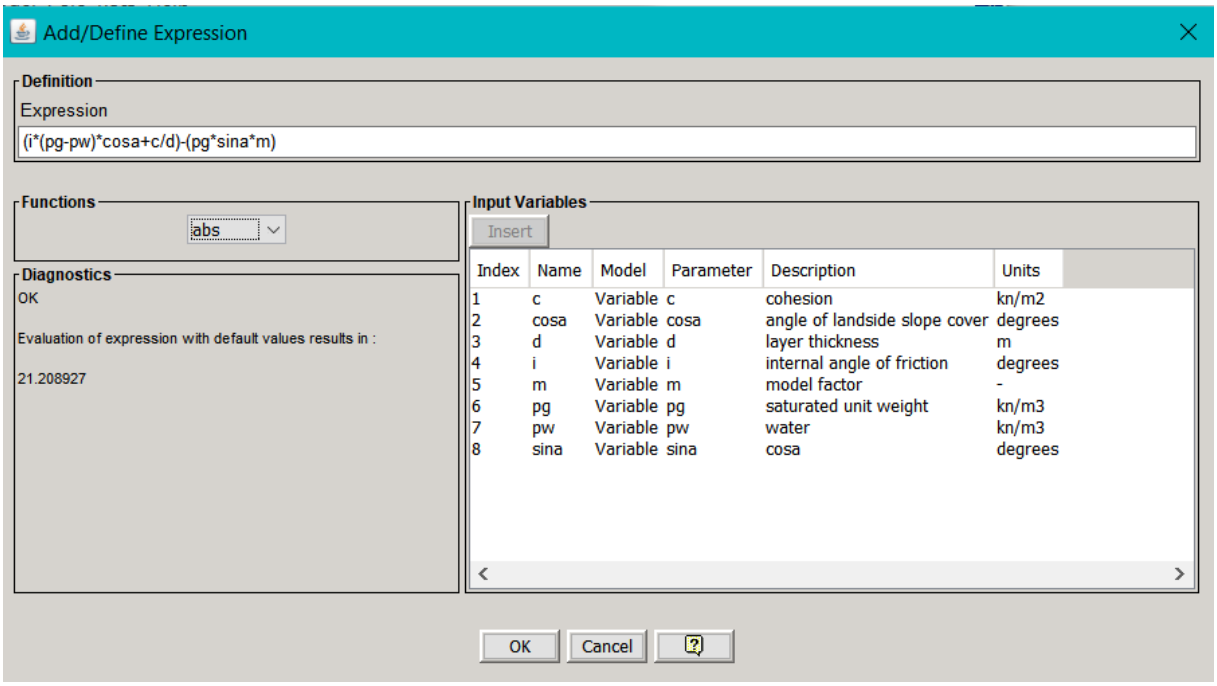

Figure 34 Prob2B Z-function

4. The results from the FORM calculation for one case are given in Figure 35, where the Beta is the reliability index and alfa the influence coefficients.

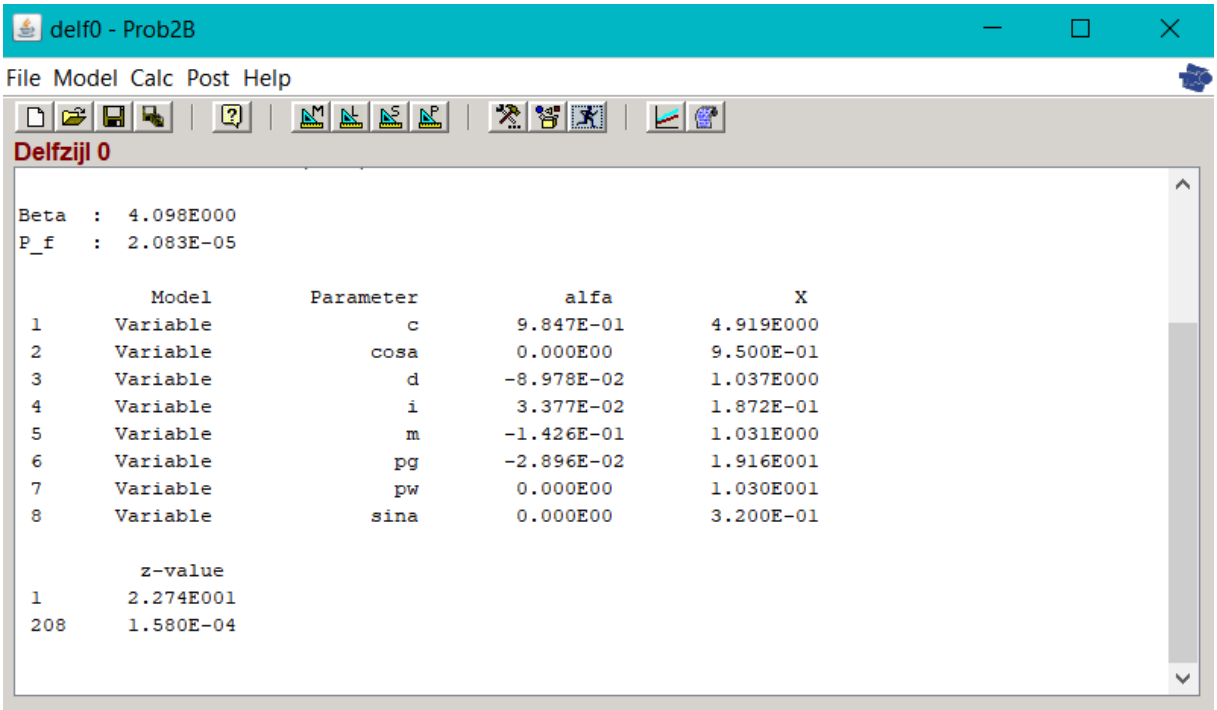

Figure 35 Prob2B results FORM calculation

5. The results from the Monte Carlo Simulation for one case are given in Figure 36, where the beta is the reliability index and alfa the influence coefficient.

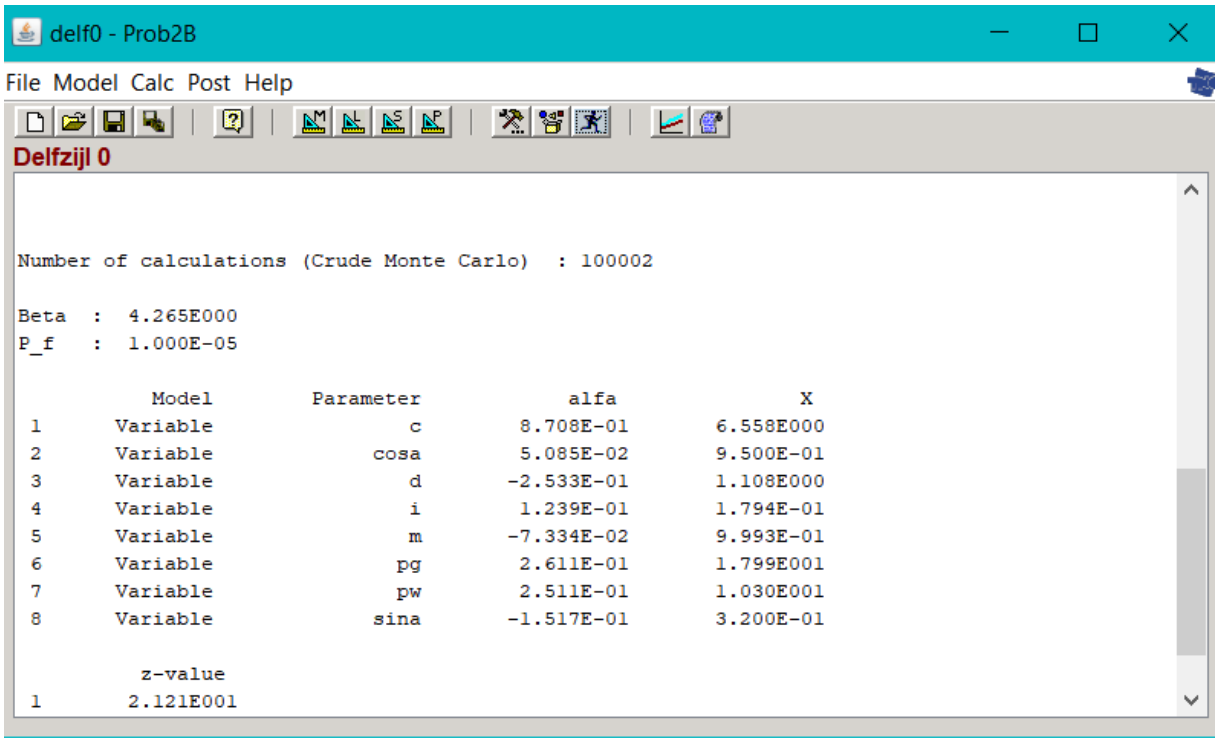

Figure 36 The Prob2B results from the Crude Monte Carlo simulation

E. Spencer-Van der Meij vs. Bishop

The stability calculation of Spencer-Van der Meij is more sensitive to user schematization errors and therefore is checked with the Bishop calculation. The stability factors of Spencer-Van der Meij & Bishop are situated on the x-axis and the stability factor of the Edelman & Joustra formula on the y-axis. As can be seen in Figure 37 the stability factor for Spencer-Van der Meij is for all cases lower than the stability factor of Bishop.

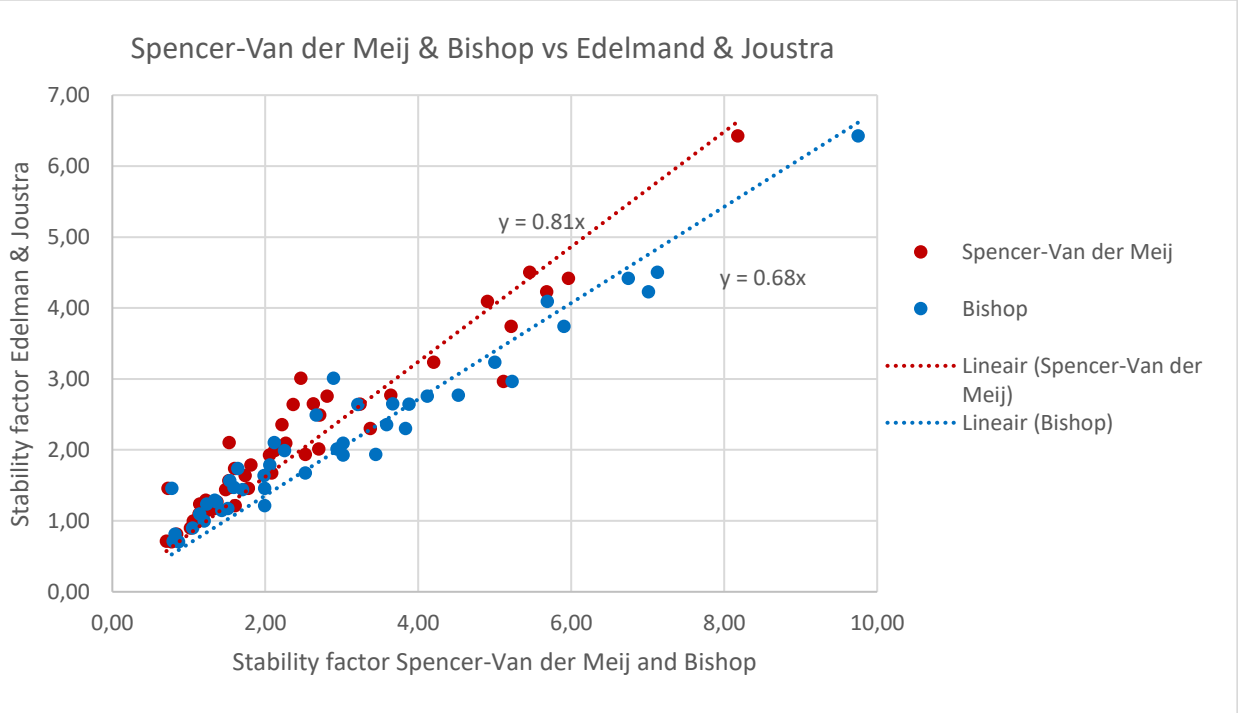

Figure 37 Difference between Bishop and Spencer-Van der Meij

F. Reliability index with respect to the values of the parameters

The reliability index from the probabilistic FORM analysis is plotted for each parameter value. The reliability index is plotted on the x-axis and the parameter value on the y-axis as can be seen in Figure 38.

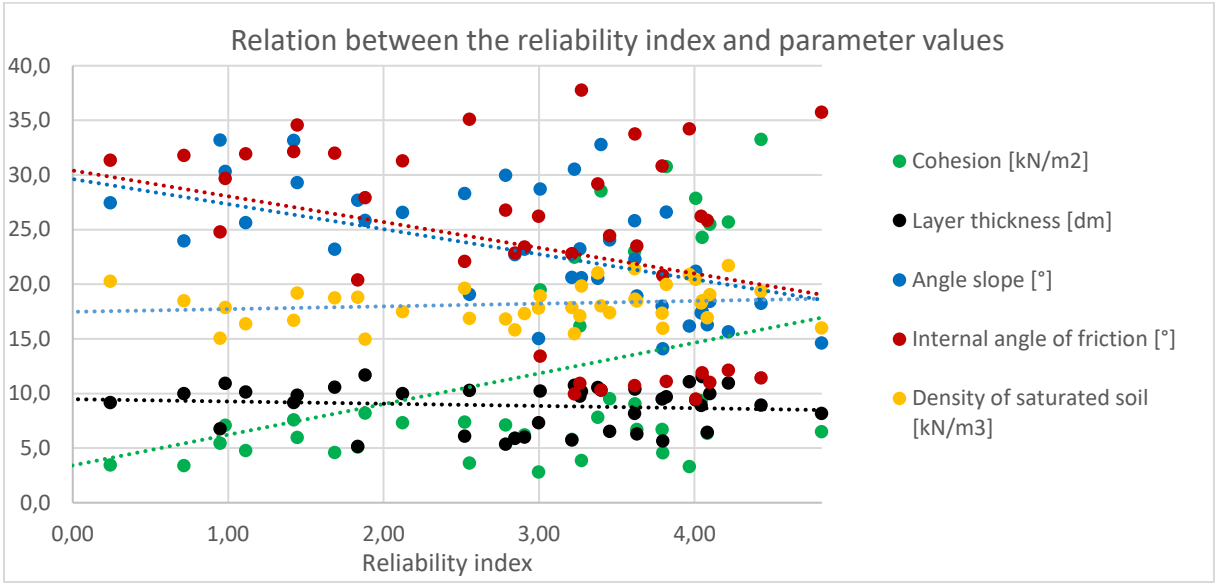

Figure 38 Reliability index with respect to the values of the parameters

G. Calibration of the safety-dependent partial safety factor

The reliability index from the FORM calculation is plotted on the x-axis and the stability factor of the Edelman & Joustra formula with the new safety in-depended factors is plotted on the y-axis as can be seen in Figure 39.

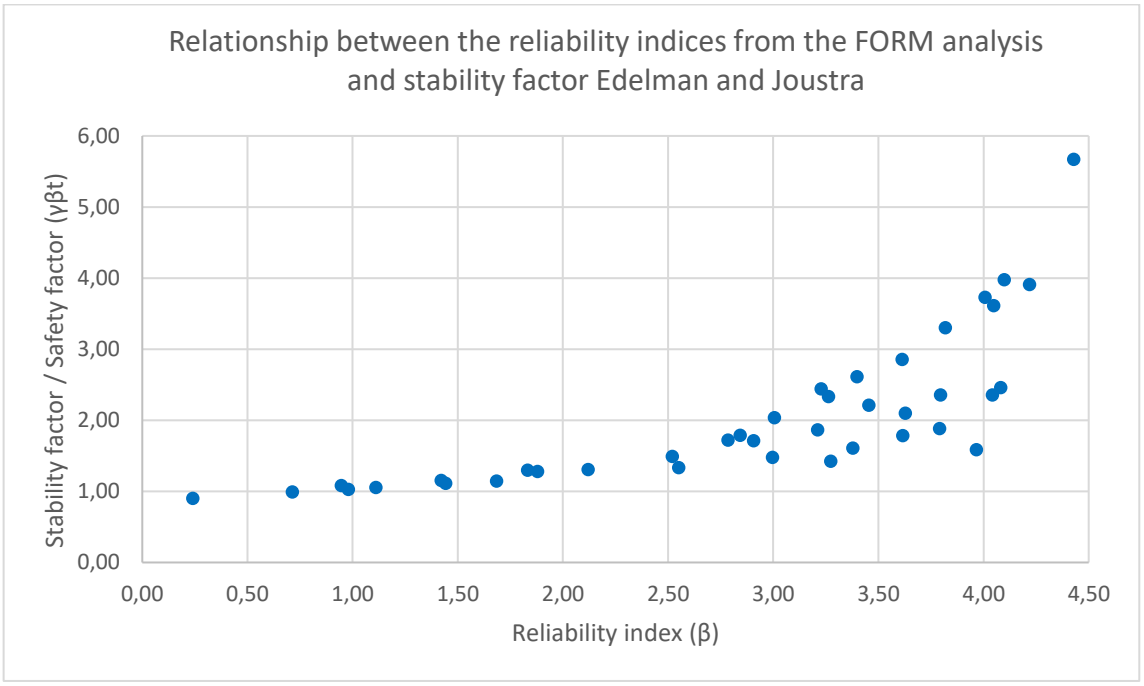

Figure 39 Relation between the stability factor and the Reliability index for all cases

In Figure 40 the relation is shown between the stability factor of Edelman & Joustra with the new partial safety factors on the y-axis and the reliability index from the probabilistic FORM analysis on the x-axis. With the method of least squared differences, an 80% best fit line is fitted through the points.

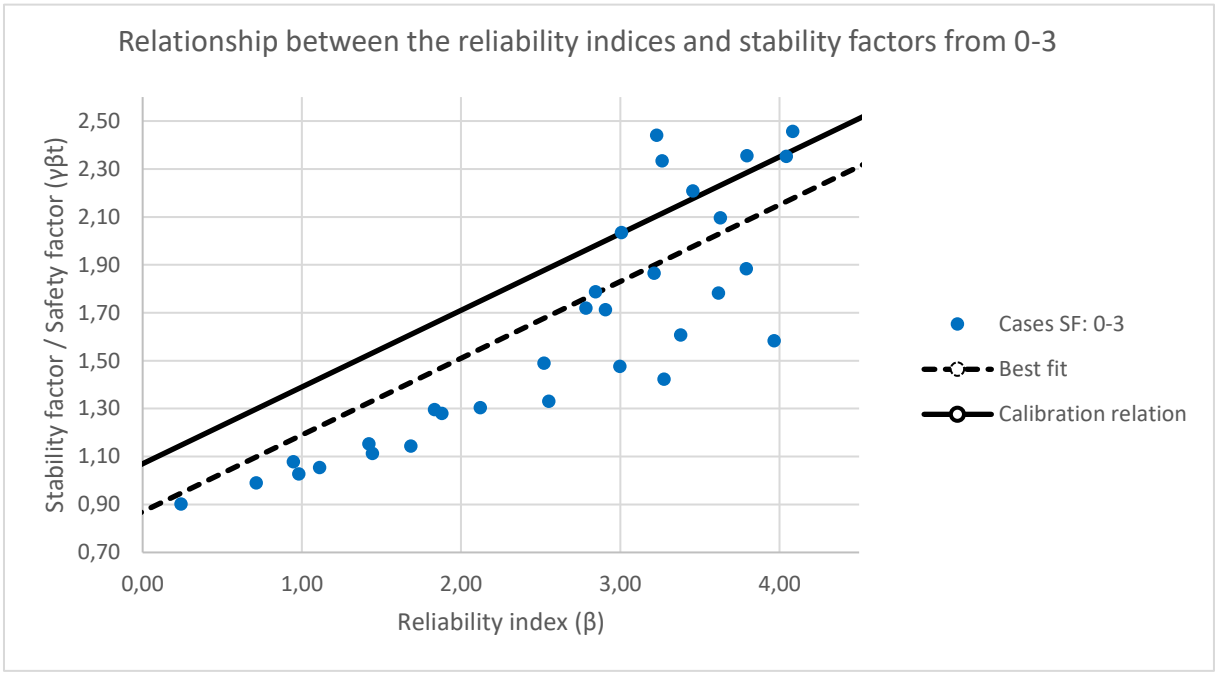

Figure 40 Calibration of the safety depended partial safety factor for stability factor between 0-3.

In Figure 41 the relation is shown between the stability factor of Edelman & Joustra with the new partial safety factors on the y-axis and the reliability index from the probabilistic FORM analysis on the x-axis. With the method of least squared differences, an 80% best fit line is fitted through the points.

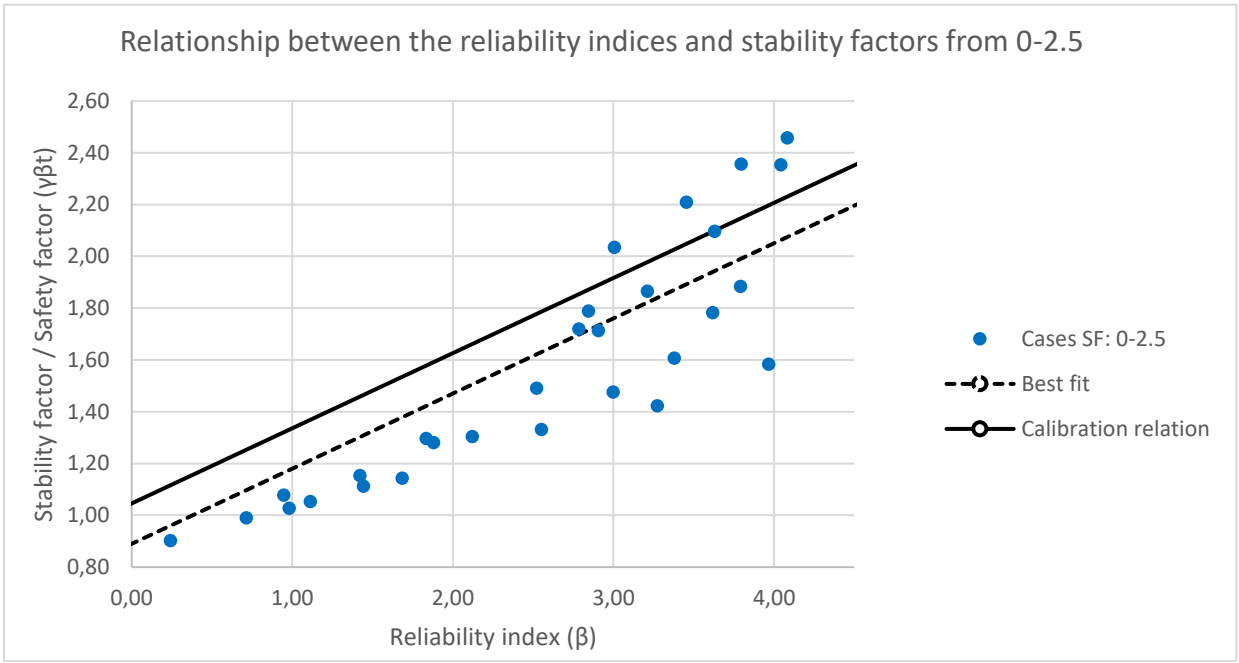

Figure 41 Calibration of the safety depended partial safety factor for stability factor between 0-2.5.

In Figure 42 the relation is shown between the stability factor of Edelman & Joustra with the new partial safety factors on the y-axis and the reliability index from the probabilistic FORM analysis on the x-axis. With the method of least squared differences an 80% best fit line is fitted through the points.

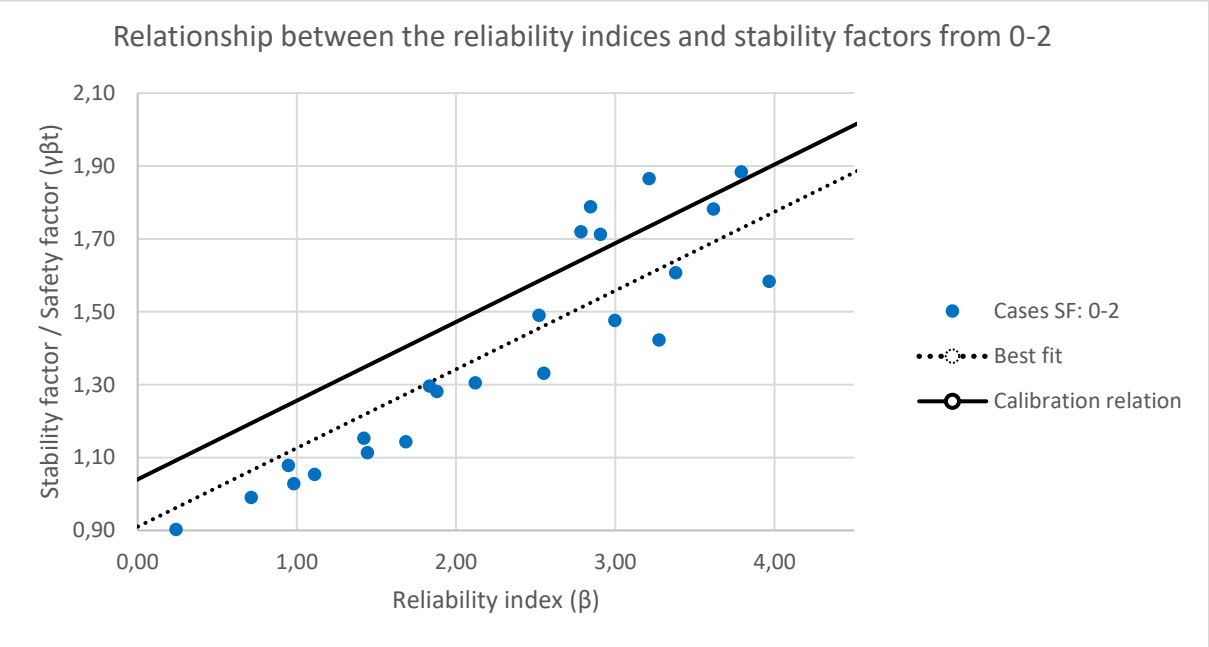

Figure 42 Calibration of the safety depended partial safety factor for stability factor between 0-2.

In Figure 43 the relation is shown between the stability factor of Edelman & Joustra with the new partial safety factors on the y-axis and the reliability index from the probabilistic FORM analysis on the x-axis. With the method of least squared differences an 80% best fit line is fitted through the points.

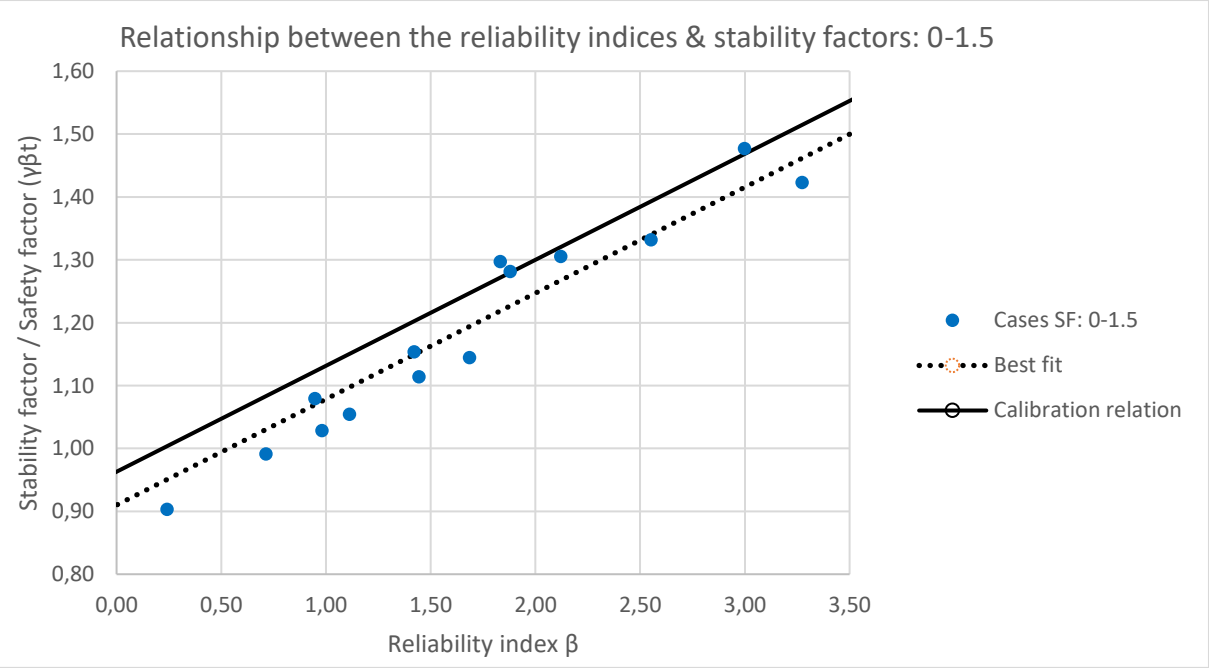

Figure 43 Calibration of the safety depended partial safety factor for stability factor between 0-1.5.

H. Reviewing the developed assessment

The developed method is compared with the current method by assessing the stability of the 44 cases. The new method takes into account the exceedance probability of a critical discharge of 1.0 l/s/m, the length effect, the trajectory norm, and the failure budget. The safety requirement for the infiltration location is applied to all 10 synthetic cases. The number of cases that are assessed as sufficient are plotted on the x-axis and the failure budget on the x-axis. The semi-probabilistic assessment is overestimating the probabilistic assessment with a failure budget smaller than 5% but is sufficiently safe larger than 5%. The calibration relation with an SF 0-2.5 has the best fit with respect to the probabilistic assessment as can be seen in Figure 44.

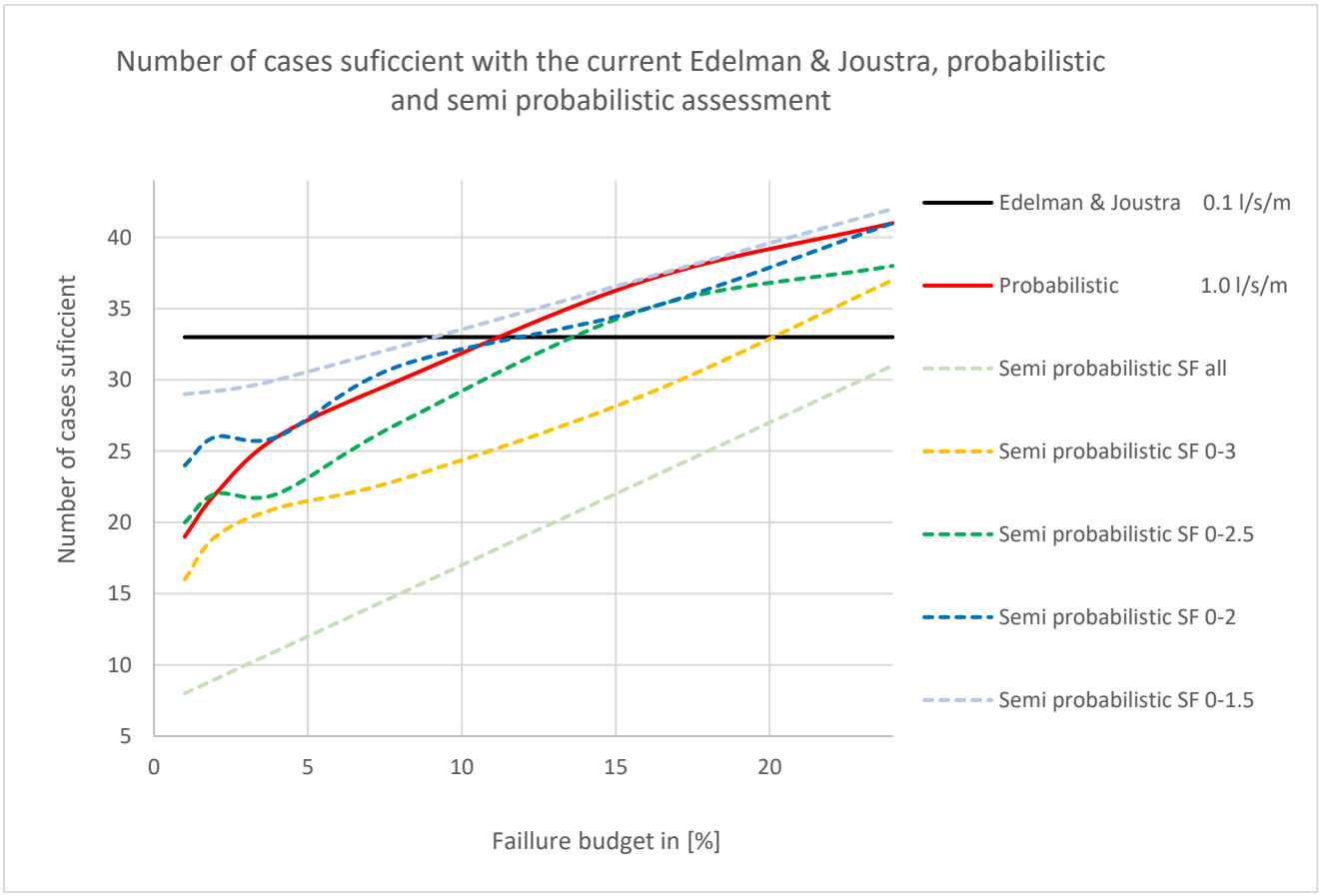

Figure 44 Outcome of the current-, the semi-probabilistic and the probabilistic assessment as a function of the failure budget